

Evolutionary Many-Objective Optimization Based on Adversarial Decomposition

Mengyuan Wu¹, Ke Li², Sam Kwong¹, and Qingfu Zhang¹

¹Department of Computer Science, City University of Hong Kong

²College of Engineering, Mathematics and Physical Sciences, University of Exeter

*Email: k.li@exeter.ac.uk, mengyuan.wu@my.cityu.edu.hk, cssamk, qingfu.zhang@cityu.edu.hk

Abstract: The decomposition-based method has been recognized as a major approach for multi-objective optimization. It decomposes a multi-objective optimization problem into several single-objective optimization subproblems, each of which is usually defined as a scalarizing function using a weight vector. Due to the characteristics of the contour line of a particular scalarizing function, the performance of the decomposition-based method strongly depends on the Pareto front's shape by merely using a single scalarizing function, especially when facing a large number of objectives. To improve the flexibility of the decomposition-based method, this paper develops an adversarial decomposition method that leverages the complementary characteristics of two different scalarizing functions within a single paradigm. More specifically, we maintain two co-evolving populations simultaneously by using different scalarizing functions. In order to avoid allocating redundant computational resources to the same region of the Pareto front, we stably match these two co-evolving populations into one-one solution pairs according to their working regions of the Pareto front. Then, each solution pair can at most contribute one mating parent during the mating selection process. Comparing with nine state-of-the-art many-objective optimizers, we have witnessed the competitive performance of our proposed algorithm on 130 many-objective test instances with various characteristics and Pareto front's shapes.

Keywords: Many-objective optimization, evolutionary algorithm, stable matching theory, decomposition-based method.

1 Introduction

Many real-life disciplines (e.g., optimal design [1], economics [2] and water management [3]) often involve optimization problems having multiple conflicting objectives, known as multi-objective optimization problems (MOPs). Rather than a global optimum that optimizes all objectives simultaneously, in multi-objective optimization, decision makers often look for a set of Pareto-optimal solutions which consist of the best trade-offs among conflicting objectives. The balance between convergence and diversity is the cornerstone of multi-objective optimization. In particular, the convergence means the approximation to the Pareto-optimal set should be as close as possible; while the diversity means the spread of the trade-off solutions should be as uniform as possible.

Evolutionary algorithm, which in principle can approximate the Pareto-optimal set in a single run, has been widely accepted as a major approach for multi-objective optimization [4]. Over the past three decades, many efforts have been devoted in developing evolutionary multi-objective optimization (EMO) algorithms and have obtained recognized performance on problems with two or three objectives [5–12]. With the development of science and technology, real-life optimization scenarios bring more significant challenges, e.g., complicated landscape, multi-modality and high dimensionality, to the algorithm design. As reported in [13–15], the performance of traditional EMO algorithms severely deteriorate with the increase of the number of objectives. Generally speaking,

researchers owe the performance deterioration to three major reasons, i.e., the loss of selection pressure for Pareto domination [14], the difficulty of density estimation in a high-dimensional space [16] and its anti-convergence phenomenon [17], and the exponentially increased computational complexity [18].

As a remedy to the loss of selection pressure for Pareto domination in a high-dimensional space, many modified dominance relationships have been developed to strengthen the comparability between solutions, e.g., ϵ -dominance [19], fuzzy Pareto-dominance [20], k -optimality [21], preference order ranking [22], control of dominance area [23] and grid dominance [24]. Very recently, a generalized Pareto-optimality was developed in [25] to expand the dominance area of Pareto domination, so that the percentage of non-dominated solutions in a population does not increase dramatically with the number of objectives. Different from [23], the expansion envelop for all solutions are kept the same in [25]. Other than the Pareto dominance-based approaches, L -optimality was proposed in [26] to help rank the solutions.

The loss of selection pressure can also be remedied by an effective diversity maintenance strategy. To relieve the anti-convergence phenomenon, [17] applied the maximum spread indicator developed in [27] to activate and deactivate the diversity promotion mechanism in NSGA-II [5]. To facilitate the density estimation in a high-dimensional space, [16] proposed to replace the crowding distance used in NSGA-II by counting the number of associated solutions with regard to a predefined reference point. In particular, a solution is considered being associated with a reference point if it has the shortest perpendicular distance to this reference point. Instead of handling the convergence and the diversity separately, [28] proposed to co-evolve a set of target vectors, each of which represents a optimization goal. The fitness value of a solution is defined by aggregating the number of current goals it achieves, i.e., dominates. The population diversity is implicitly maintained by the goals widely spread in the objective space; while the selection pressure towards the convergence is strengthened by co-evolving the optimization goals with the population.

The exponentially increased computational costs come from two aspects: 1) the exponentially increased computational complexity for calculating the hypervolume, which significantly hinders the scalability of the indicator-based EMO algorithms; 2) the significantly increased computational costs for maintaining the non-domination levels [5] of a large number of solutions in a high-dimensional space. As for the former aspect, some improved methods, from the perspective of computational geometry [29–31] or Monte carlo sampling [18], have been proposed to enhance the efficiency of hypervolume calculation. As for the latter aspect, many efforts have been devoted to applying some advanced data structures to improve the efficiency of non-dominated sorting procedure [32–34]. It is worth noting that our recent study [35] showed that it can be more efficient to update the non-domination levels by leveraging the population structure than to sort the population from scratch in every iteration.

As reported in [36–38], decomposition-based EMO methods have become increasingly popular for solving problems with more than three objectives, which are often referred to as many-objective optimization problems (MaOPs). Since the decomposition-based EMO methods transform an MOP into several single-objective optimization subproblems, it does not suffer the loss of selection pressure of Pareto domination in a high-dimensional space. In addition, the update of the population relies on the comparison of the fitness values, thus the computational costs do not excessively increase with the dimensionality. As reported in [39], different subproblems, which focus on different regions in the objective space, have various difficulties. Some superior solutions can easily dominantly occupy several subproblems. This is obviously harmful to the population diversity and getting worse with the increase of the dimensionality. To overcome this issue, [40] built an interrelationship between subproblems and solutions, where each subproblem can only be updated by its related solutions. Based on the similar merit, [41] restricted a solution to only updating one of its K closest subproblems. In [42], two metrics were proposed to measure the convergence and diversity separately. More specifically, the objective vector of a solution is at first projected onto its closest weight vector. Then, the distance between the projected point and the ideal point measures the solution’s convergence; while the distance between the projected point and the original objective vector measures the solution’s diversity. At the end, a diversity-first update scheme was developed

according to these two metrics. Analogously, [43] developed a modified achievement scalarizing function as the convergence metric while an angle-based density estimation method was employed to measure the solution’s diversity.

Recently, there is a growing trend in leveraging the advantages of the decomposition- and Pareto-based methods within the same framework. For example, [44] suggested to use the Pareto domination to prescreen the population. The local density is estimated by the number of solutions associated with a pre-defined weight vector. In particular, a solution located in an isolated region has a higher chance to survive to the next iteration. Differently, [45] developed an angle-based method to estimate the local crowdedness around a weight vector. In addition to the density estimation, the weight vectors divide the objective space into different subspaces, which is finally used to estimate the local strength value [6] of each solution. Analogously, in [46], a non-dominated sorting is conducted upon all the subspaces, where solutions in different subspaces are considered non-dominated to each other. [47] developed a dual-population paradigm which co-evolves two populations simultaneously. These populations are maintained by different selection mechanisms respectively, while their interaction is implemented by a restricted mating selection mechanism.

Although the decomposition-based EMO methods have been extensively used for MaOPs, a recent comprehensive study [38] demonstrated that the performance of decomposition-based EMO methods strongly depends on the shape of the Pareto front (PF). This phenomenon can be attributed to two major reasons:

- Most, if not all, decomposition-based EMO methods merely consider a single scalarizing function in fitness assignment. Since the contour line of a scalarizing function does not adapt to a particular problem’s characteristic, the flexibility is restricted.
- As discussed in the previous paragraph, different regions of the PF have various difficulties. The balance between convergence and diversity of the search process can be easily biased by some dominantly superior solutions. The increasing dimensionality exacerbates this phenomenon.

Bearing the above considerations in mind, this paper develops a new decomposition-based method, called adversarial decomposition, for many-objective optimization. Generally speaking, it has the following three features:

- It maintains two co-evolving populations simultaneously, each of which is maintained by a different scalarizing function. In particular, one population uses the boundary intersection-based scalarizing function, while the other one applies a modified achievement scalarizing function. In this regard, the search behaviors of these two populations become different, where one is convergence-oriented while the other is diversity-oriented.
- In order to make these two populations complement each other, they use ideal and nadir points respectively as the reference point in their scalarizing functions. By doing this, the two populations are evolved following two sets of adversarial search directions.
- During the mating selection process, two populations are at first stably matched to form a set of one-one solution pairs. In particular, solutions within the same pair concentrate on similar regions of the PF. Thereafter, each solution pair can at most contribute one mating parent for offspring generation. By doing this, we can expect an uniformly spread of the computational efforts over the entire PF.

The remainder of this paper is organized as follows. Section 2 provides some preliminaries useful to this paper. Section 3 describes the technical details of our proposed method step by step. The empirical studies are presented and discussed in Section 4 and Section 5. Finally, Section 6 concludes the paper and provides some future directions.

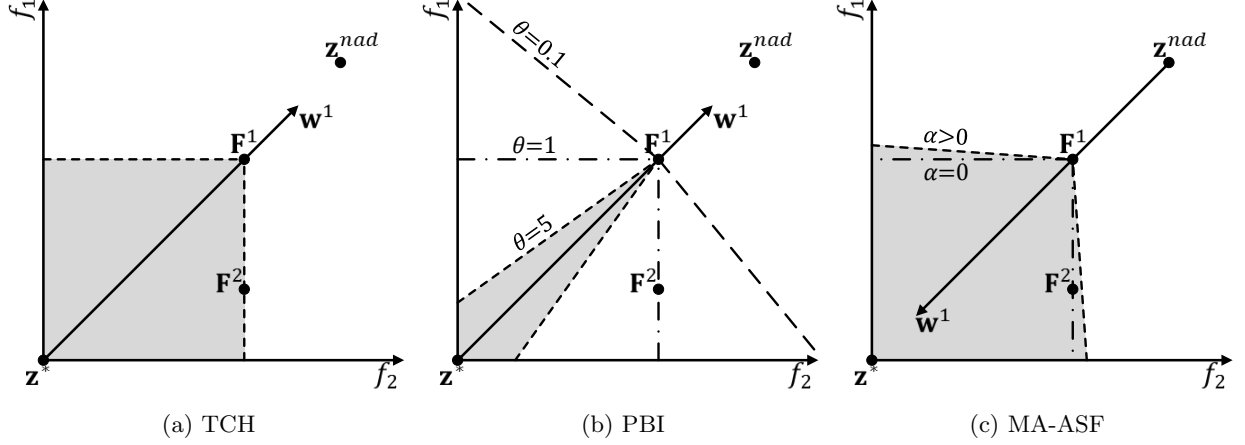


Figure 1: Illustration of the characteristics of different scalarizing functions.

2 Preliminaries

This section first provides some basic definitions of multi-objective optimization. Afterwards, we briefly introduce the decomposition of multi-objective optimization.

2.1 Basic Definitions

The MOP considered in this paper can be mathematically defined as follows:

$$\begin{aligned} & \text{minimize} && \mathbf{F}(\mathbf{x}) = (f_1(\mathbf{x}), \dots, f_m(\mathbf{x}))^T \\ & \text{subject to} && \mathbf{x} \in \Omega \end{aligned}, \quad (1)$$

where $\mathbf{x} = (x_1, \dots, x_n)^T \in \Omega$ is a n -dimensional decision variable vector from the decision space \mathbb{R}^n and $\mathbf{F}(\mathbf{x})$ is a m -dimensional objective vector in the objective space \mathbb{R}^m .

Definition 1. Given solutions $\mathbf{x}^1, \mathbf{x}^2 \in \Omega$, \mathbf{x}^1 is said to dominate \mathbf{x}^2 , denoted by $\mathbf{x}^1 \preceq \mathbf{x}^2$, if and only if $f_i(\mathbf{x}^1) \leq f_i(\mathbf{x}^2)$ for all $i \in \{1, \dots, m\}$ and $\mathbf{F}(\mathbf{x}^1) \neq \mathbf{F}(\mathbf{x}^2)$.

Definition 2. A solution $\mathbf{x} \in \Omega$ is called Pareto-optimal if and only if there is no other solution dominates it.

Definition 3. The Pareto-optimal set (PS) is defined as the set of all Pareto-optimal solutions. Their corresponding objective vectors form the Pareto-optimal front (PF).

Definition 4. The ideal point is $\mathbf{z}^* = (z_1^*, \dots, z_m^*)^T$, where $z_i^* = \min_{\mathbf{x} \in \Omega} \{f_i(\mathbf{x})\}$ for all $i \in \{1, \dots, m\}$. The nadir point is $\mathbf{z}^{nad} = (z_1^{nad}, \dots, z_m^{nad})^T$, where $z_i^{nad} = \max_{\mathbf{x} \in \Omega} \{f_i(\mathbf{x})\}$.

2.2 Decomposition

Under some mild conditions, the task of approximating the PF can be decomposed into several scalar optimization subproblems, each of which is formed by a weighted aggregation of all individual objectives [48]. In the classic multi-objective optimization literature [49], there have been several established approaches for constructing scalarizing functions, among which the weighted Tchebycheff (TCH) and penalty-based boundary intersection (PBI) [48] are the most popular ones. More specifically, the TCH function is mathematically defined as:

$$\begin{aligned} & \text{minimize} && g^{tch}(\mathbf{x}|\mathbf{w}, \mathbf{z}^*) = \max_{1 \leq i \leq m} \{|f_i(\mathbf{x}) - z_i^*|/w_i\} \\ & \text{subject to} && \mathbf{x} \in \Omega \end{aligned}, \quad (2)$$

where $\mathbf{w} = (w^1, \dots, w^m)^T$ is a user specified weight vector, $w_i \geq 0$ for all $i \in \{1, \dots, m\}$ and $\sum_{i=1}^m w_i = 1$. Note that w_i is set to be a very small number, say 10^{-6} , in case $w_i = 0$. The contour line of the TCH function is shown in Fig. 1(a) where $\mathbf{w} = (0.5, 0.5)^T$. From this figure, we can clearly see that the control area (i.e., the area that holds better solutions) of the TCH function is similar to the Pareto domination defined in Definition 1, e.g., solutions located in the gray shaded area (i.e., the control area of \mathbf{F}^1) are better than \mathbf{F}^1 . Note that the TCH function cannot discriminate the *weakly* dominated solution [49]. For example, the TCH function values of \mathbf{F}^1 and \mathbf{F}^2 are the same, but $\mathbf{F}^1 \preceq \mathbf{F}^2$ according to Definition 1.

As for the PBI function, it is mathematically defined as:

$$\begin{aligned} \text{minimize } & g^{pbi}(\mathbf{x}|\mathbf{w}, \mathbf{z}^*) = d_1(\mathbf{F}(\mathbf{x})|\mathbf{w}, \mathbf{z}^*) \\ & + \theta d_2(\mathbf{F}(\mathbf{x})|\mathbf{w}, \mathbf{z}^*) , \\ \text{subject to } & \mathbf{x} \in \Omega \end{aligned} \quad (3)$$

where

$$\begin{aligned} d_1(\mathbf{y}|\mathbf{w}, \mathbf{z}) &= \frac{\|(\mathbf{y} - \mathbf{z})^T \mathbf{w}\|}{\|\mathbf{w}\|} \\ d_2(\mathbf{y}|\mathbf{w}, \mathbf{z}) &= \left\| \mathbf{y} - \left(\mathbf{z} + \frac{d_1}{\|\mathbf{w}\|} \mathbf{w} \right) \right\| . \end{aligned} \quad (4)$$

As discussed in [44], d_1 and d_2 measure the convergence and diversity of \mathbf{x} with regard to \mathbf{w} , respectively. The balance between convergence and diversity is parameterized by θ , which also controls the contour line of the PBI function. In Fig. 1(b), we present the contour lines of PBI functions with different θ settings.

3 Many-Objective Optimization Algorithm Based on Adversarial Decomposition

In this section, we introduce the technical details of our proposed many-objective optimization algorithm based on adversarial decomposition, denoted as MOEA/AD whose pseudo code is given in Algorithm 1, step by step. At the beginning, we initialize a population of solutions $S = \{\mathbf{x}^1, \dots, \mathbf{x}^N\}$ via random sampling upon Ω ; the ideal and nadir points; a set of weight vectors $W = \{\mathbf{w}^1, \dots, \mathbf{w}^N\}$ and build their neighborhood structure according to the method in [44]. Afterwards, we assign S directly to the two co-evolving populations, i.e., diversity population S_d and convergence population S_c . Note that S_d and S_c share the same weight vectors, each of which corresponds to a unique subproblem for S_d and S_c respectively. To facilitate the mating selection process, we initialize a matching array M and a sentinel array R , where $M[i]$ indicates a solution \mathbf{x}_d^i in S_d is paired with a solution $\mathbf{x}_c^{M[i]}$ in S_c and $R[i]$ indicates whether this pair of solutions work in similar regions of the PF. During the main while loop, the mating parents are selected from the solution pairs. The generated offspring solution is used to update S_d and S_c separately. After each generation, we divide the solutions in $S_d \cup S_c$ into different solution pairs for the next round's mating selection process. The major components of MOEA/AD are explained in the following subsections.

3.1 Adversarial Decomposition

As discussed in Section 1, the flexibility of the decomposition-based method is restricted due to the use of a single scalarizing function. Bearing this consideration in mind, this paper develops an adversarial decomposition method. Its basic idea is to maintain two co-evolving and complementary populations simultaneously, each of which is maintained by a different scalarizing function.

More specifically, one population is maintained by the PBI function introduced in Section 2.2, where we set $\theta = 5.0$ as recommended in [44]. The other population is maintained by a modified

Algorithm 1: MOEA/AD

Input: algorithm parameters
Output: final population S_c and S_d

- 1 Initialize a set of solutions S , \mathbf{z}^* and \mathbf{z}^{nad} ;
- 2 Initialize a set of weight vectors W and its neighborhood structure B ;
- 3 $S_c \leftarrow S$, $S_d \leftarrow S$;
- 4 **for** $i \leftarrow 1$ **to** N **do**
- 5 $M[i] \leftarrow i$, $R[i] \leftarrow 1$;
- 6 $generation \leftarrow 0$;
- 7 **while** *Stopping criterion is not satisfied* **do**
- 8 **for** $i \leftarrow 1$ **to** N **do**
- 9 $\bar{S} \leftarrow \text{MatingSelection}(S_c, S_d, i, M, R, W, B)$;
- 10 $\bar{\mathbf{x}} \leftarrow \text{Variation}(\bar{S})$;
- 11 Update \mathbf{z}^* and \mathbf{z}^{nad} ;
- 12 $(S_c, S_d) \leftarrow \text{PopulationUpdate}(S_c, S_d, \bar{\mathbf{x}}, W)$;
- 13 $(M, R) \leftarrow \text{Match}(S_c, W)$;
- 14 $generation++$;
- 15 **return** S_c, S_d ;

augmented achievement scalarizing function (MA-ASF) defined as follows:

$$\begin{aligned} \text{minimize } g^c(\mathbf{x}|\mathbf{w}, \mathbf{z}^{nad}) &= \max_{1 \leq i \leq m} \{(f_i(\mathbf{x}) - z_i^{nad})/w_i\} \\ &\quad + \alpha \sum_{i=1}^m (f_i(\mathbf{x}) - z_i^{nad})/w_i \quad , \end{aligned} \quad (5)$$

subject to $\mathbf{x} \in \Omega$

where α is an augmentation coefficient. Comparing with the TCH function in equation (2), the MA-ASF uses the nadir point to replace the ideal point and the absolute operator is removed to allow $f_i(\mathbf{x})$ to be smaller than z_i^{nad} , where $i \in \{1, \dots, m\}$. Furthermore, the augmentation term in the MA-ASF helps avoid weakly Pareto-optimal solutions. As shown in Fig. 1(c), the contour line of the MA-ASF is the same as that of the TCH function in case $\alpha = 0$; while the control area of the MA-ASF becomes wider when setting $\alpha > 0$. In this case, the MA-ASF is able to discriminate the weakly dominated solution, e.g., the MA-ASF value of \mathbf{F}^2 in Fig. 1(c) is better than that of \mathbf{F}^1 when $\alpha > 0$. Here we use a sufficiently small $\alpha = 10^{-6}$ as recommended in [50].

To deal with problems having different scales of objectives, we normalize the objective values before using the scalarizing function. By doing this, the PBI function becomes:

$$\bar{g}^d(\mathbf{x}|\mathbf{w}) = d_1(\bar{\mathbf{F}}(\mathbf{x})|\mathbf{w}, \mathbf{0}) + \theta d_2(\bar{\mathbf{F}}(\mathbf{x})|\mathbf{w}, \mathbf{0}), \quad (6)$$

where $\bar{\mathbf{F}}(\mathbf{x}) = (\bar{f}_1(\mathbf{x}), \dots, \bar{f}_m(\mathbf{x}))^T$ and $\bar{f}_i(\mathbf{x}) = \frac{f_i(\mathbf{x}) - z_i^*}{z_i^{nad} - z_i^*}$ for all $i \in \{1, \dots, m\}$. The MA-ASF is re-written as:

$$\begin{aligned} \bar{g}^c(\mathbf{x}|\mathbf{w}) &= \max_{1 \leq i \leq m} \{(\bar{f}_i(\mathbf{x}) - 1)/w_i\} \\ &\quad + \alpha \sum_{i=1}^m (\bar{f}_i(\mathbf{x}) - 1)/w_i \quad . \end{aligned} \quad (7)$$

In the following paragraphs, we will discuss the complementary effects achieved by the PBI function and MA-ASF.

- As shown in Fig. 1(b) and Fig. 1(c), the control areas of the PBI function with $\theta = 5.0$ is much narrower than that of the MA-ASF. In this case, the population is driven towards the

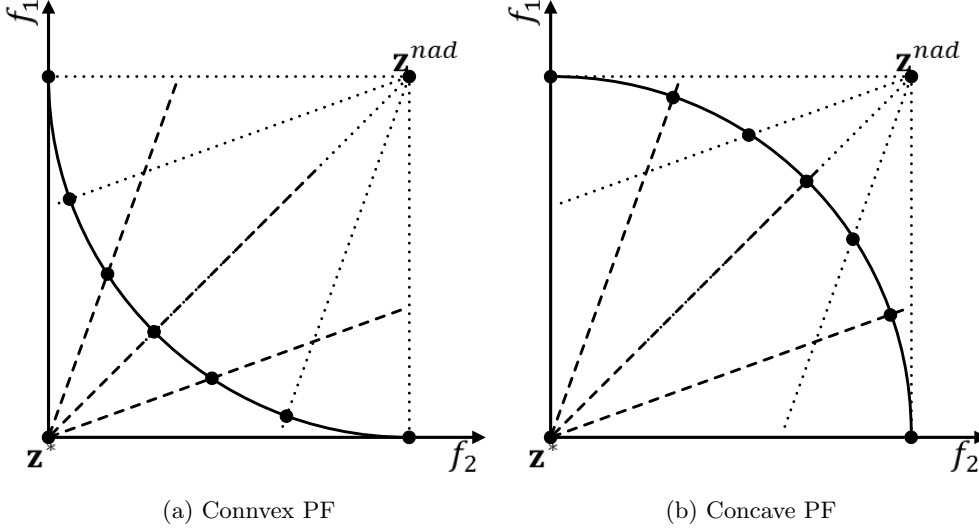


Figure 2: Illustration of the complementary effects achieved by adversarial search directions on the convex and concave PFs.

corresponding weight vector by using the PBI function as the selection criteria. Moreover, comparing to the MA-ASF, the control areas shared by different weight vectors are smaller in the PBI function. Accordingly, various weight vectors have a larger chance to hold different elite solutions and we can expect an improvement on the population diversity. On the other hand, due to the narrower control area, the selection pressure, with regard to the convergence, of the PBI function is not as strong as the MA-ASF. In other words, some solutions, which can update the subproblem maintained by a MA-ASF, might not be able to update the subproblem maintained by a PBI function. For example, as shown in Fig. 1(b), although $\mathbf{F}^2 \preceq \mathbf{F}^1$, the PBI function value of \mathbf{F}^2 is worse than that of \mathbf{F}^1 with regard to \mathbf{w}^1 . In this case, the PBI function has a high risk of compromising the population convergence.

- The other reason, which results in the different behaviors of the PBI function and MA-ASF, is their adversarial search directions by using the ideal point and nadir point respectively. More specifically, the PBI function pushes solutions toward the ideal point as close as possible; while the MA-ASF pushes the solutions away from the nadir point as far as possible. Therefore, given the same set of weight vectors, the search regions of the PBI function and MA-ASF complement each other. For example, for a convex PF shown in Fig. 2(a), solutions found by the PBI function using the ideal point concentrate on the central region of the PF; in contrast, those found by the MA-ASF using the nadir point fill the gap between the central region and the boundary. As for a concave PF shown in Fig. 2(b), solutions found by the PBI function using the ideal point sparsely spread over the PF; while those found by the MA-ASF using the nadir point improve the population diversity.

In summary, by using the scalarizing functions introduced above, i.e., the PBI function and the MA-ASF, the adversarial decomposition method makes the two co-evolving populations become complementary, i.e., one is diversity-oriented (denoted as the diversity population S_d) and the other is convergence-oriented (denoted as the convergence population S_c). In addition, the search regions is also diversified so that the solutions are able to cover a wider range of the PF.

3.2 Population Update

After the generation of an offspring solution $\bar{\mathbf{x}}$, it is used to update S_d and S_c separately. Note that the optimal solution for each subproblem is assumed to be along its corresponding reference line that connects the origin and the weight vector [40]. Thus, to make S_d as diversified as possible,

Algorithm 2: PopulationUpdate($S_c, S_d, \bar{\mathbf{x}}, W$)

Input: S_c, S_d, W and an offspring solution $\bar{\mathbf{x}}$ **Output:** Updated S_c and S_d

```
1 for  $i \leftarrow 1$  to  $N$  do
2    $D_d[i] \leftarrow d_2(\bar{F}(\bar{\mathbf{x}})|\mathbf{w}^i, \mathbf{0})$ ;
3    $i_d \leftarrow \underset{0 \leq i \leq N}{\operatorname{argmin}} D_d[i]$ 
4   if  $\bar{g}^d(\bar{\mathbf{x}}|\mathbf{w}^{i_d}) \leq \bar{g}^d(\mathbf{x}_d^{i_d}|\mathbf{w}^{i_d})$  then
5      $\mathbf{x}_d^{i_d} \leftarrow \bar{\mathbf{x}}$ ;
6   for  $i \leftarrow 1$  to  $N$  do
7      $D_c[i] \leftarrow d_2(\bar{F}(\bar{\mathbf{x}})|\mathbf{w}^i, \mathbf{1})$ ;
8    $I_c \leftarrow$  Sort  $D_c$  in ascending order and return the indexes;
9    $t \leftarrow 0$ ;
10  for  $i \leftarrow 1$  to  $N$  do
11    if  $\bar{g}^c(\bar{\mathbf{x}}|\mathbf{w}^{I_c[i]}) \leq \bar{g}^c(\mathbf{x}_c^{I_c[i]}|\mathbf{w}^{I_c[i]})$  then
12       $\mathbf{x}_c^{I_c[i]} \leftarrow \bar{\mathbf{x}}, t++$ ;
13       $\mathbf{x}_c^{I_c[i]}.closeness \leftarrow i, \mathbf{x}_c^{I_c[i]}.closestP \leftarrow I_c[0]$ ;
14      if  $t == nr_c$  then
15        break;
16 return  $S_c, S_d$ ;
```

we expect that different subproblems can hold different elite solutions. In this case, we restrict $\bar{\mathbf{x}}$ to only updating its closest subproblem (as shown in line 1 to line 5 of Algorithm 2). As for S_c , its major purpose is to propel the population to the PF. To accelerate the convergence progress, we allow a dominantly superior solution to take over more than one subproblem, say $nr_c \geq 1$. In particular, we at first sort the priorities of different subproblems according to their distances to $\bar{\mathbf{x}}$. It can update its nr_c closest subproblems in case $\bar{\mathbf{x}}$ has a better MA-ASF function value (as shown line 6 to line 15 of Algorithm 2). It is worth noting that we reserve two additional terms, in line 13 of Algorithm 2, to facilitate the mating selection procedure introduced in Section 3.3.2. One is the degree of closeness of the updated solution to its corresponding subproblem, denoted as *closeness*; the other is the index of this solution's closest subproblem, denoted as *closestP*.

3.3 Mating Selection and Reproduction

The interaction between the two co-evolving populations is an essential step in algorithms that consider multiple populations [47, 51]. To take advantage of the complementary effects between S_d and S_c , the interaction is implemented as a restricted mating selection mechanism that chooses the mating parents according to their working regions. Generally speaking, it contains two consecutive steps: one is the pairing step that makes each solution in S_d be paired with a solution in S_c ; the other is the mating selection step that selects the appropriate parents for the offspring reproduction. We will illustrate them in detail as follows.

3.3.1 Pairing Step

To facilitate the latter mating selection step, the pairing step divides the two populations into different solution pairs, each of which contains two solutions from S_d and S_c respectively. This is achieved by finding a one-one stable matching between the solutions in S_d and S_c . As a result, solutions in the same pair are regarded to have a similar working regions of the PF.

To find a stable matching between solutions in S_d and S_c , we need to define their mutual preferences at first. Specifically, since each solution in S_d is close to its corresponding subproblem,

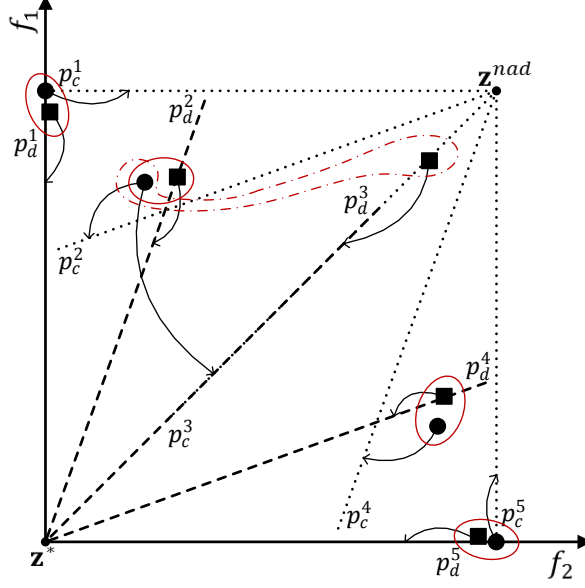


Figure 3: Illustration of a pairing result. p_d^i and p_c^i , $i \in \{1, \dots, 5\}$, indicate the subproblem in S_d and S_c , respectively. The association of a solution and a subproblem is represented as an arrow.

we define the preference of a solution in S_d (denoted as \mathbf{x}_d) to a solution in S_c (denoted as \mathbf{x}_c) as:

$$\Delta_{DC}(\mathbf{x}_d, \mathbf{x}_c) = \bar{g}^d(\mathbf{x}_c | \mathbf{w}_d), \quad (8)$$

where \mathbf{w}_d is the weight vector of the subproblem occupied by \mathbf{x}_d . As for the preference of \mathbf{x}_c to \mathbf{x}_d , it is defined as:

$$\Delta_{CD}(\mathbf{x}_c, \mathbf{x}_d) = d_2(\bar{F}(\mathbf{x}_c) | \mathbf{w}_d, \mathbf{0}). \quad (9)$$

Then, we sort the preference list of each solution in an ascending order and apply our recently developed two-level one-one stable matching method [52, 53] to find a stable matching. Note that the two-level stable matching method is able to match each agent with one of its most preferred partners. Since a solution of an m -objective problem always locates within the local area between m closest weight vectors, the length of the preference list is reduced to m in the first-level matching process [53]. As a result, the matched solutions in the first-level stable matching should work on the similar regions of the PF. For example, as shown in Fig. 3, the solution pairs formed in the first-level stable matching are surrounded by the red solid curves. From this figure, we can see that these matched solutions are close to each other and work on the similar regions. Therefore, we set the corresponding index of a sentinel array R to 1, i.e., $R[i] = 1$ where $i \in \{1, 2, 4, 5\}$ and denote the corresponding subproblems have collaborative information. During the second-level matching process, the remaining solutions are matched based on the complete preference lists. Note that the matched solutions in the second-level stable matching are not guaranteed to work on the similar regions any longer. As shown in Fig. 3, the solution pair formed in second-level stable matching, surrounded by the red dotted curve, are away from each other. Thus, we set $R[3] = 0$. The pseudo code of this pairing step is presented in Algorithm 3.

3.3.2 Mating Selection Step

The mating parents consist of two parts: one is the principal parent; the others are from its neighbors. Note that each solution pair is only allowed to contribute at most one mating parent to avoid wasting the computational resources upon the similar regions. Given a solution pair $(\mathbf{x}_d^i, \mathbf{x}_c^{M[i]})$, the first step is to decide the population from which the principal parent is selected. This depends on the following three criteria.

Algorithm 3: Match(S_c, W)

Input: S_c, W **Output:** Matching array M and sentinel array R

```
1 Calculate preference lists for  $S_c$  and  $P_d$ ;  
2 Compute a two-level stable matching between  $S_c$  and  $P_d$ ;  
3 for  $i \leftarrow 1$  to  $N$  do  
4    $M[i] \leftarrow$  Index of the matching mate in  $S_c$  of  $\mathbf{x}_d^i$ ;  
5   if  $\mathbf{x}_d^i$  finds a stable matching mate in the first-level stable matching then  
6      $R[i] \leftarrow 1$ ; // the  $i$ -th subproblem has collaborative information  
7   else  
8      $R[i] \leftarrow 0$ ;  
9 return  $M, R$ 
```

- The first criterion is the *subproblem's relative improvement*. As for \mathbf{x}_d^i , it is defined as:

$$\Delta_d^i = \frac{\bar{g}^d(\mathbf{x}_d^{i,old} | \mathbf{w}^i) - \bar{g}^d(\mathbf{x}_d^{i,new} | \mathbf{w}^i)}{\bar{g}^d(\mathbf{x}_d^{i,old} | \mathbf{w}^i)}, \quad (10)$$

where $\mathbf{x}_d^{i,new}$ and $\mathbf{x}_d^{i,old}$ are respectively the current and previous solution of the i th subproblem in S_d , respectively. As for $\mathbf{x}_c^{M[i]}$, it is defined as:

$$\Delta_c^{M[i]} = \left| \frac{\bar{g}^c(\mathbf{x}_c^{M[i],old} | \mathbf{w}^{M[i]}) - \bar{g}^c(\mathbf{x}_c^{M[i],new} | \mathbf{w}^{M[i]})}{\bar{g}^c(\mathbf{x}_c^{M[i],old} | \mathbf{w}^{M[i]})} \right|. \quad (11)$$

If Δ_d^i and $\Delta_c^{M[i]}$ are in a tie, we need the following two secondary criteria for decision making.

- As discussed in Section 3.1, a solution found by the PBI function is not guaranteed to be non-dominated. If \mathbf{x}_d^i is dominated by a solution in $S_d \cup S_c$, it is inappropriate to be chosen as a mating parent.
- As discussed in Section 3.2, a dominantly superior solution can occupy more than one subproblem by considering the MA-ASF. In this case, such solution may occupy a subproblem away from its working region, which makes it inadequate to be a mating parent.

The pseudo code of the principal parent selection mechanism is given in Algorithm 4. If the subproblem's relative improvement of \mathbf{x}_d^i is larger than that of $\mathbf{x}_c^{M[i]}$, it means that the corresponding subproblem of \mathbf{x}_d^i has a higher potential for further improvement. And the principal parent should be selected from S_d , i.e., \mathbf{x}_d^i . Otherwise, $\mathbf{x}_c^{M[i]}$ will be chosen as the principal parent (line 1 to line 4 of Algorithm 4). If Δ_d^i and $\Delta_c^{M[i]}$ are in a tie, we need to check the domination status of \mathbf{x}_d^i and $\mathbf{x}_c^{M[i]}$'s closeness to the corresponding subproblem (line 6 to line 11 of Algorithm 4). By comparing the subproblems' relative improvements, we can expect an efficient allocation of the computational resources to different regions of the PF. The two secondary criteria implicitly push the solutions towards the corresponding weight vectors thus improve the population diversity.

After the selection of the principal parent, the other mating parent are selected from the neighbors of the subproblem occupied by the principal parent. More specifically, if the principal parent is from S_d , we store the solutions of its neighboring subproblems from both S_d and S_c into a temporary mating pool S_p . Note that only those subproblems having collaborative information (i.e., $R[i] = 1$) are considered when choosing solutions from S_c (line 5 and line 8 of Algorithm 5). On the other hand, if the principal parent is from S_c , only solutions from S_c have the chance to be stored in S_p . Note that we do not consider the solution that has the same closest subproblem as the principal parent (line 12 and line 14 of Algorithm 5). Once S_p is set up, the other mating parents are randomly chosen from it.

Algorithm 4: PopSelection(S_c, S_d, i, M, W)

Input: S_c, S_d, W , matching array M and the subproblem index i **Output:** population index pop

```
1 if  $\Delta_d^i > \Delta_c^{M[i]}$  then
2   |  $pop \leftarrow 1;$  // chosen from  $S_d$ 
3 else if  $\Delta_d^i < \Delta_c^{M[i]}$  then
4   |  $pop \leftarrow 2;$  // chosen from  $S_c$ 
5 else
6   | if  $\mathbf{x}_d^i$  is nondominated and  $\mathbf{x}_c^{M[i]}$ .closeness  $> m$  then
7     |  $pop \leftarrow 1;$ 
8   | else if  $\mathbf{x}_d^i$  is dominated and  $\mathbf{x}_c^{M[i]}$ .closeness  $\leq m$  then
9     |  $pop \leftarrow 2;$ 
10  | else
11  |  $pop \leftarrow$  Randomly select from  $\{1, 2\};$ 
12 return  $pop;$ 
```

Algorithm 5: MatingSelection(S_c, S_d, i, M, R, W, B)

Input: S_c, S_d, W , matching array M and the subproblem index i , sentinel array R , neighborhood structure B **Output:** mating parents \bar{S}

```
1  $pop \leftarrow$  PopSelection( $S_c, S_d, i, M, W$ );
2 if  $rand < \delta$  then
3   |  $S_p \leftarrow \emptyset;$ 
4   | if  $pop == 1$  then
5     | for  $j \leftarrow 1$  to  $T$  do
6       |  $S_p \leftarrow S_p \cup \{\mathbf{x}_d^{B[i][j]}\};$ 
7       | if  $R[B[i][j]] == 1$  then
8         |  $S_p \leftarrow S_p \cup \{\mathbf{x}_c^{M[B[i][j]]}\};$ 
9       |  $\mathbf{x}^r \leftarrow$  Randomly select a solution from  $S_p;$ 
10      |  $\bar{S} \leftarrow \{\mathbf{x}_d^i, \mathbf{x}^r\};$ 
11   | else
12     | for  $j \leftarrow 1$  to  $T$  do
13       | if  $\mathbf{x}_c^{B[M[i][j]]}$ .closestP  $\neq \mathbf{x}_c^{M[i]}$ .closestP then
14         |  $S_p \leftarrow S_p \cup \{\mathbf{x}_c^{B[M[i][j]]}\};$ 
15       |  $\mathbf{x}^r \leftarrow$  Randomly select a solution from  $S_p;$ 
16       |  $\bar{S} \leftarrow \{\mathbf{x}_c^{M[i]}, \mathbf{x}^r\};$ 
17   | else
18     |  $S_p \leftarrow S_c \cup S_d;$ 
19     |  $\mathbf{x}^r \leftarrow$  Randomly select a solution from  $S_p;$ 
20     | if  $pop == 1$  then
21       |  $\bar{S} \leftarrow \{\mathbf{x}_d^i, \mathbf{x}^r\};$ 
22     | else
23       |  $\bar{S} \leftarrow \{\mathbf{x}_c^{M[i]}, \mathbf{x}^r\};$ 
24 return  $\bar{S}$ 
```

This paper uses the simulated binary crossover (SBX) [54] and polynomial mutation [55] for offspring generation. The mating parents are treated, while only one offspring solution will be randomly chosen for updating S_d and S_c .

4 Experimental Setup

In this section, we describe the setup of our empirical studies, including the benchmark problems, performance indicator, peer algorithms and their parameter settings.

4.1 Benchmark Problems

Here we choose DTLZ1 to DTLZ4 [56], WFG1 to WFG9 [57], and their minus version proposed in [58], i.e., DTLZ1⁻¹ to DTLZ4⁻¹ and WFG1⁻¹ to WFG9⁻¹ to form the benchmark problems in our empirical studies. In particular, the number of objectives are set as $m \in \{3, 5, 8, 10, 15\}$. The number of decision variables of DTLZ and DTLZ⁻¹ problem instances [56] is set to $n = m + k + 1$, where $k = 5$ for DTLZ1 and DTLZ1⁻¹ and $k = 10$ for the others. As for WFG and WFG⁻¹ problem instances [57], we set $n = k + l$, where $k = 2 \times (m - 1)$ and $l = 20$. Note that the DTLZ and WFG benchmark problems have been widely used for benchmarking the performance of many-objective optimizers; while their minus version is proposed to investigate the resilience to the irregular PF shapes. All these benchmark problems are scalable to any number of objectives.

4.2 Performance Indicator

In our empirical studies, we choose the widely used Hypervolume (HV) indicator [59] to quantitatively evaluate the performance of a many-objective optimizer. Specifically, the HV indicator is calculated as:

$$HV(S) = \text{VOL}\left(\bigcup_{\mathbf{x} \in S} [f_1(\mathbf{x}), z_1^r] \times \cdots \times [f_m(\mathbf{x}), z_m^r]\right), \quad (12)$$

where S is the solution set, $\mathbf{z}^r = (z_1^r, \dots, z_m^r)$ is a point dominated by all Pareto-optimal objective vectors and VOL indicates the Lebesgue measure. In our empirical studies, we set $\mathbf{z}^r = (2, \dots, 2)^T$ and the objective vectors are normalized to $[0, 1]$ before calculating the HV. The larger the HV value is, the better the quality of S is for approximating the true PF. Each algorithm is run 31 times independently and the Wilcoxon's rank sum test at 5% significant level is performed to show whether the peer algorithm is significantly outperformed by our proposed MOEA/AD. Note that we choose the population that has the higher HV value as the output of our proposed MOEA/AD.

4.3 Peer Algorithms

Here we choose nine state-of-the-art many-objective optimizers to validate the competitiveness of our proposed MOEA/AD. These peer algorithms belong to different types, including two decomposition-based algorithms (MOEA/D [48] and Global WASF-GA [60]), two Pareto-based algorithms (PICEA-g [28] and VaEA [61]), two indicator-based algorithms (HypE [18] and KnEA [62]), two algorithms that integrates the decomposition- and Pareto-based selection together (NSGA-III [16] and θ -DEA [46]), and an improved two-archive-based algorithm (Two_Arch2 [63]). Some further comments upon the peer algorithms are listed as follows.

- *MOEA/D* uses the original PBI function with $\theta = 5.0$ for the DTLZ and WFG problem instances. As for the DTLZ⁻¹ and WFG⁻¹ problem instances, it uses the inverted PBI function [64] with $\theta = 0.1$ as suggested in [58]. Note that the inverted PBI function replaces the ideal point with the nadir point in equation (3).
- *Global WASF-GA* is a decomposition-based algorithm that selects solutions to survive according to the rankings of solutions to each subproblem. Similar to MOEA/AD, it uses the ideal

Table 1: Settings of the Number of Generations.

Problem Instance	$m=3$	$m=5$	$m=8$	$m=10$	$m=15$
DTLZ1, DTLZ1 ⁻¹	400	600	750	1,000	1,500
DTLZ2, DTLZ2 ⁻¹	250	350	500	750	1,000
DTLZ3, DTLZ3 ⁻¹	1,000	1,000	1,000	1,500	2,000
DTLZ4, DTLZ4 ⁻¹	600	1,000	1,250	2,000	3,000
WFG, WFG ⁻¹	400	750	1,500	2,000	3,000

point and nadir point simultaneously in its scalarizing function. However, instead of maintaining two co-evolving populations, Global WASF-GA only has a single population, where half of it are maintained by the scalarizing function using the ideal point while the other are maintained by the nadir point.

- *PICEA-g* co-evolves a set of target vectors sampled in the objective space, which can be regarded as a second population and is used to guide the environmental selection.
- *Two_Arch2* maintains two archives via indicator-based selection and Pareto-based selection separately. In particular, an L_p -norm-based diversity maintenance scheme is designed to maintain the diversity archive.

4.4 Parameter Settings

- *Weight vector*: We employ the method developed in [44] to generate the weight vectors used in the MOEA/D variants. Note that we add an additional weight vector $\{1/m, \dots, 1/m\}$ to remedy the missing the centroid on the simplex for the 8-, 10- and 15-objective cases.
- *Population size*: We set the population size the same as the number of weight vectors. In particular, N is set as 91, 210, 157, 276 and 136 for $m = \{3, 5, 8, 10, 15\}$ respectively.
- *Termination criteria*: As suggested in [16], the termination criterion is set as a predefined number of generations, as shown in Table 1.
- *Reproduction operators*: For the SBX, we set the crossover probability p_c to 1.0 and the distribution index η_c to 30 [16]. As for the polynomial mutation, the probability p_m and distribution index η_m are set to be $1/n$ and 20 [16], respectively.
- *Neighborhood size*: $T = 20$ [48].
- *Probability to select in the neighborhood*: $\delta = 0.9$ [48].

The intrinsic parameters of the other peer algorithms are set according to the recommendations in their original papers.

5 Empirical Studies

In this section, we present and discuss the comparison results of our proposed MOEA/AD with the other state-of-the-art peer algorithms. The mean HV values are given in Table 2 to Table 6, where the best results are highlighted in boldface with a gray background.

5.1 Comparisons on DTLZ and WFG Problem Instances

Generally speaking, MOEA/AD is the most competitive algorithm for the DTLZ problem instances. As shown in Table 2, it wins in 161 out of 180 comparisons. More specifically, for DTLZ1 and DTLZ3, MOEA/AD obtains the largest HV values on all comparisons except for the 15-objective

Table 2: Comparison Results of MOEA/AD and 9 Peer Algorithms on DTLZ Problem Instances.

Problem	m	PBI	GWASF	PICEA-g	VaEA	HypE	KnEA	NSGA-III	θ -DEA	TwoArch2	MOEA/AD
DTLZ1	3	7.785e+0 [†]	7.134e+0 [†]	7.562e+0 [†]	7.764e+0 [†]	7.774e+0 [†]	7.307e+0 [†]	7.786e+0	7.738e+0 [†]	7.785e+0 [†]	7.787e+0
	5	3.197e+1 [†]	1.965e+1 [†]	3.191e+1 [†]	3.194e+1 [†]	3.186e+1 [†]	2.939e+1 [†]	3.197e+1 [†]	3.197e+1 [†]	3.196e+1 [†]	3.197e+1
	8	2.560e+2 [†]	7.026e+1 [†]	2.482e+2 [†]	2.559e+2 [†]	1.973e+2 [†]	1.739e+2 [†]	2.560e+2	2.560e+2 [†]	2.559e+2 [†]	2.560e+2
	10	1.024e+3 [†]	4.761e+2 [†]	1.010e+3 [†]	1.024e+3 [†]	9.573e+2 [†]	8.514e+2 [†]	1.024e+3 [†]	1.024e+3 [†]	1.024e+3 [†]	1.024e+3
	15	3.275e+4	1.092e+3 [†]	2.815e+4 [†]	3.275e+4 [‡]	0.000e+0 [†]	2.621e+4 [†]	3.276e+4[‡]	3.264e+4 [‡]	3.275e+4	3.270e+4
DTLZ2	3	7.413e+0[‡]	7.301e+0 [†]	7.376e+0 [†]	7.405e+0 [†]	7.371e+0 [†]	7.393e+0 [†]	7.412e+0	7.413e+0 [‡]	7.407e+0 [†]	7.412e+0
	5	3.170e+1	3.037e+1 [†]	3.165e+1 [†]	3.166e+1 [†]	3.117e+1 [†]	3.166e+1 [†]	3.169e+1 [†]	3.170e+1 [†]	3.161e+1 [†]	3.170e+1
	8	2.558e+2 [†]	2.423e+2 [†]	2.551e+2 [†]	2.558e+2 [†]	2.525e+2 [†]	2.558e+2 [†]	2.558e+2 [†]	2.558e+2 [†]	2.554e+2 [†]	2.558e+2
	10	1.024e+3 [†]	6.398e+2 [†]	1.023e+3 [†]	1.024e+3 [†]	1.017e+3 [†]	1.024e+3 [†]	1.024e+3 [†]	1.024e+3 [†]	1.022e+3 [†]	1.024e+3
	15	3.276e+4	1.638e+4 [†]	3.231e+4 [†]	3.276e+4	3.207e+4 [†]	3.277e+4	3.276e+4	3.276e+4	3.275e+4 [†]	3.276e+4
DTLZ3	3	7.406e+0 [‡]	6.504e+0 [†]	6.849e+0 [†]	7.401e+0	7.285e+0 [†]	7.236e+0 [†]	7.406e+0	7.403e+0	7.413e+0[‡]	7.403e+0
	5	3.169e+1	1.600e+1 [†]	2.997e+1 [†]	3.166e+1 [†]	1.332e+1 [†]	2.862e+1 [†]	3.169e+1 [†]	3.169e+1 [†]	3.159e+1 [†]	3.169e+1
	8	2.459e+2 [†]	1.278e+2 [†]	2.081e+2 [†]	2.237e+2 [†]	0.000e+0 [†]	1.542e+2 [†]	2.558e+2	2.558e+2	2.542e+2 [†]	2.558e+2
	10	1.024e+3 [†]	5.115e+2 [†]	9.394e+2 [†]	9.219e+2 [†]	0.000e+0 [†]	7.105e+2 [†]	1.024e+3 [†]	9.805e+2 [†]	1.020e+3 [†]	1.024e+3
	15	2.328e+4 [†]	1.631e+4 [†]	2.422e+4 [†]	2.674e+4 [†]	0.000e+0 [†]	0.000e+0 [†]	3.276e+4	2.380e+4 [†]	3.256e+4 [†]	3.276e+4
DTLZ4	3	6.398e+0 [†]	6.961e+0 [†]	7.053e+0 [†]	7.408e+0 [†]	7.414e+0[‡]	7.396e+0 [†]	7.059e+0 [†]	7.243e+0 [†]	7.069e+0 [†]	7.412e+0
	5	3.087e+1 [†]	2.710e+1 [†]	3.144e+1 [†]	3.167e+1 [†]	3.149e+1 [†]	3.167e+1 [†]	3.170e+1 [‡]	3.170e+1[‡]	3.161e+1 [†]	3.169e+1
	8	2.547e+2 [†]	1.575e+2 [†]	2.552e+2 [†]	2.558e+2 [†]	2.471e+2 [†]	2.558e+2 [†]	2.558e+2	2.558e+2	2.551e+2 [†]	2.558e+2
	10	1.023e+3 [†]	7.165e+2 [†]	1.023e+3 [†]	1.024e+3 [†]	1.019e+3 [†]	1.024e+3 [†]	1.024e+3	1.024e+3	1.022e+3 [†]	1.024e+3
	15	3.276e+4 [†]	1.636e+4 [†]	3.254e+4 [†]	3.276e+4 [†]	3.262e+4 [†]	3.277e+4[‡]	3.276e+4 [†]	3.276e+4	3.274e+4 [†]	3.276e+4

According to Wilcoxon's rank sum test, [†] and [‡] indicates whether the corresponding algorithm is significantly worse or better than MOEA/AD respectively.

DTLZ1 and the 3-objective DTLZ3 instances. As for DTLZ2, MOEA/D-PBI obtains the best HV value on the 3-objective case, while MOEA/AD takes the leading position when the number of objectives becomes large. For DTLZ4, the best algorithm varies with different number of objectives. Even though MOEA/AD loses in 4 out of 45 comparisons, the differences are very slight. In addition, as for two decomposition-based algorithms, MOEA/D-PBI obtains significantly worse HV values than MOEA/AD on 14 out of 20 comparisons, while Global WASF-GA were significantly outperformed on all 20 comparisons. In particular, Global WASF-GA fails to approximate the entire PF on all DTLZ instances due to its coarse diversity maintenance scheme. As for the two recently proposed Pareto-based many-objective optimizers, the HV values obtained by PICEA-g are significantly worse than MOEA/AD on all problem instances. This can be explained by its randomly sampled target vectors which slow down the convergence speed. VaEA performs slightly better than PICEA-g but it is still outperformed by MOEA/AD on 18 out of 20 comparisons. As expected, the performance of two indicator-based algorithms are not satisfied. In particular, KnEA merely obtains the best HV values on the 15-objective DTLZ2 and DTLZ4 instances. θ -DEA and NSGA-III, which combine the decomposition- and Pareto-based selection methods together, achieve significantly better results than MOEA/AD in 2 and 3 comparisons respectively, where MOEA/AD beats them in 9 and 11 comparisons respectively. Two_Arch2, which also maintains two co-evolving populations, is significantly outperformed by MOEA/AD on all DTLZ instances except for the 15-objective DTLZ1 and the 3-objective DTLZ3. Given these observations, we find that the genuine performance obtained by MOEA/AD does not merely come from the two co-evolving populations. The adversarial search directions and their collaborations help strike the balance between convergence and diversity.

The comparison results on WFG problem instances are given in Table 3. From these results, we can see that MOEA/AD shows the best performance on all WFG4, WFG5, WFG7 and WFG8 instances when the number of objectives is larger than 3, where it wins in 143 out of 144 comparisons. For WFG6, although MOEA/AD only wins on the 10-objective case, its worse performance on the other WFG6 instances are not statistically significant. KnEA obtains the largest HV values on all WFG9 instances. As for WFG1 to WFG3, which have irregular PFs, Two_Arch2 shows the best performance on 12 instances. In contrast, MOEA/AD only obtains the best HV results on 3- and 5-objective WFG1 instances. It is worth noting that NSGA-III, KnEA, PICEA-g and VaEA perform quite well on the WFG2 instances. Due to irregular PFs, the decomposition-based algorithms struggle to find a nondominated solution for each subproblem, while Two_Arch2 together with the above four algorithms are still able to allocate all computational resources upon the PF. Nevertheless, HypE cannot perform as good as KnEA. Talking about the other algorithms, WASF-GA and MOEA/D-PBI give the worst overall performance. Unlike on the DTLZ problem instances, the performance MOEA/D-PBI degrades a lot on the WFG instances. In contrast, by simultaneously

Table 3: Comparison Results of MOEA/AD and 9 Peer Algorithms on WFG Problem Instances.

Problem	m	PBI	GWASF	PICEA-g	VaEA	HypE	KnEA	NSGA-III	θ -DEA	TwoArch2	MOEA/AD
WFG1	3	5.515e+0 [†]	6.031e+0 [†]	5.277e+0 [†]	5.317e+0 [†]	3.739e+0 [†]	5.380e+0 [†]	4.455e+0 [†]	5.317e+0 [†]	6.287e+0 [†]	6.355e+0
	5	2.780e+1 [†]	2.756e+1 [†]	2.449e+1 [†]	2.005e+1 [†]	1.580e+1 [†]	2.050e+1 [†]	1.737e+1 [†]	2.513e+1 [†]	2.621e+1 [†]	2.988e+1
	8	2.165e+2 [†]	1.547e+2 [†]	2.172e+2 [†]	2.172e+2 [†]	1.205e+2 [†]	1.722e+2 [†]	1.252e+2 [†]	2.314e+2	2.454e+2[‡]	2.330e+2
	10	8.402e+2 [†]	7.059e+2 [†]	9.725e+2 [‡]	9.434e+2 [†]	4.828e+2 [†]	7.520e+2 [†]	5.228e+2 [†]	9.562e+2 [†]	1.002e+3[‡]	9.673e+2
	15	2.009e+4 [†]	1.563e+4 [†]	2.746e+4 [‡]	3.040e+4 [†]	1.374e+4 [†]	2.423e+4 [†]	1.981e+4 [†]	2.263e+4 [†]	3.175e+4[‡]	2.645e+4
WFG2	3	6.832e+0 [†]	7.381e+0	7.545e+0 [‡]	7.445e+0 [†]	7.077e+0	7.519e+0 [‡]	7.423e+0 [‡]	7.557e+0 [‡]	7.637e+0[‡]	7.186e+0
	5	2.831e+1 [†]	3.083e+1 [†]	3.179e+1 [†]	3.135e+1 [†]	3.041e+1	3.166e+1 [†]	3.127e+1 [†]	3.093e+1	3.181e+1 [†]	2.954e+1
	8	2.231e+2 [†]	1.302e+2 [†]	2.497e+2 [‡]	2.503e+2 [‡]	2.388e+2 [†]	2.543e+2 [‡]	2.471e+2 [†]	2.359e+2 [†]	2.558e+2[‡]	2.435e+2
	10	9.246e+2 [†]	5.203e+2 [†]	1.010e+3 [‡]	1.019e+3 [‡]	9.801e+2 [†]	1.019e+3 [‡]	1.011e+3 [‡]	9.597e+2 [†]	1.024e+3[‡]	9.853e+2
	15	2.949e+4 [†]	1.634e+4 [†]	3.124e+4	3.195e+4 [†]	3.000e+4 [†]	3.152e+4 [†]	3.038e+4	2.592e+4 [†]	3.276e+4[‡]	3.133e+4
WFG3	3	6.348e+0 [†]	7.010e+0 [‡]	6.988e+0 [‡]	6.818e+0 [†]	6.608e+0 [†]	6.870e+0	6.889e+0 [†]	6.931e+0 [‡]	7.048e+0[‡]	6.906e+0
	5	2.484e+1 [†]	2.763e+1 [†]	2.848e+1 [‡]	2.666e+1 [†]	2.695e+1 [†]	2.615e+1 [†]	2.753e+1 [†]	2.810e+1 [†]	2.860e+1[†]	2.835e+1
	8	1.559e+2 [†]	1.278e+2 [†]	2.222e+2	2.165e+2 [†]	2.136e+2 [†]	2.065e+2 [†]	1.711e+2 [†]	1.542e+2 [†]	2.294e+2[‡]	2.219e+2
	10	4.934e+2 [†]	5.114e+2 [†]	9.010e+2 [‡]	8.670e+2 [†]	8.718e+2 [†]	8.409e+2 [†]	6.584e+2 [†]	6.066e+2 [†]	9.240e+2[‡]	8.883e+2
	15	1.340e+4 [†]	1.634e+4 [†]	2.772e+4	2.784e+4	2.700e+4 [†]	2.141e+4 [†]	1.964e+4 [†]	1.835e+4 [†]	2.946e+4[‡]	2.774e+4
WFG4	3	7.191e+0 [†]	7.246e+0 [†]	7.307e+0 [†]	7.282e+0 [†]	7.088e+0 [†]	7.324e+0 [†]	7.317e+0 [†]	7.319e+0 [†]	7.372e+0[‡]	7.369e+0
	5	3.063e+1 [†]	3.009e+1 [†]	3.135e+1 [†]	3.076e+1 [†]	2.914e+1 [†]	3.125e+1 [†]	3.107e+1 [†]	3.110e+1 [†]	3.134e+1 [†]	3.150e+1
	8	2.170e+2 [†]	1.284e+2 [†]	2.381e+2 [†]	2.513e+2 [†]	2.228e+2 [†]	2.553e+2 [†]	2.514e+2 [†]	2.520e+2 [†]	2.539e+2 [†]	2.557e+2
	10	8.608e+2 [†]	5.129e+2 [†]	9.697e+2 [†]	1.006e+3 [†]	9.242e+2 [†]	1.022e+3 [†]	1.010e+3 [†]	1.013e+3 [†]	1.018e+3 [†]	1.024e+3
	15	2.577e+4 [†]	1.638e+4 [†]	2.929e+4 [†]	3.249e+4 [†]	2.969e+4 [†]	3.273e+4 [†]	3.268e+4 [†]	3.270e+4 [†]	3.266e+4 [†]	3.274e+4
WFG5	3	7.067e+0 [†]	7.070e+0 [†]	7.090e+0 [†]	7.127e+0 [†]	6.963e+0 [†]	7.168e+0	7.130e+0 [†]	7.132e+0 [†]	7.148e+0	7.161e+0
	5	3.026e+1 [†]	2.940e+1 [†]	3.044e+1 [†]	3.024e+1 [†]	2.940e+1 [†]	3.064e+1 [†]	3.049e+1 [†]	3.053e+1 [†]	3.049e+1 [†]	3.073e+1
	8	2.310e+2 [†]	1.816e+2 [†]	2.400e+2 [†]	2.459e+2 [†]	2.146e+2 [†]	2.470e+2 [†]	2.460e+2 [†]	2.459e+2 [†]	2.451e+2 [†]	2.470e+2
	10	8.937e+2 [†]	4.735e+2 [†]	9.613e+2 [†]	9.817e+2 [†]	9.214e+2 [†]	9.866e+2 [†]	9.835e+2 [†]	9.829e+2 [†]	9.801e+2 [†]	9.867e+2
	15	2.515e+4 [†]	1.509e+4 [†]	2.924e+4 [†]	3.138e+4 [†]	2.922e+4 [†]	3.142e+4	3.141e+4 [†]	3.057e+4 [†]	3.110e+4 [†]	3.142e+4
WFG6	3	7.053e+0 [†]	7.199e+0	7.203e+0	7.169e+0 [†]	6.999e+0 [†]	7.214e+0	7.179e+0 [†]	7.190e+0 [†]	7.238e+0	7.218e+0
	5	2.896e+1 [†]	2.950e+1 [†]	3.078e+1	3.038e+1 [†]	2.990e+1 [†]	3.078e+1	3.061e+1	3.062e+1	3.074e+1	3.075e+1
	8	1.908e+2 [†]	2.478e+2	2.466e+2 [†]	2.476e+2	2.373e+2 [†]	2.481e+2	2.470e+2 [†]	2.475e+2	2.475e+2	2.479e+2
	10	7.398e+2 [†]	6.716e+2 [†]	9.906e+2 [†]	9.883e+2 [†]	9.618e+2 [†]	9.916e+2	9.880e+2 [†]	9.901e+2 [†]	9.885e+2[†]	9.941e+2
	15	1.735e+4 [†]	1.577e+4 [†]	3.060e+4 [†]	3.166e+4	3.012e+4 [†]	3.163e+4	3.161e+4	3.115e+4 [†]	3.172e+4	3.159e+4
WFG7	3	7.091e+0 [†]	7.298e+0 [†]	7.350e+0 [†]	7.330e+0 [†]	6.837e+0 [†]	7.383e+0 [†]	7.353e+0 [†]	7.363e+0 [†]	7.397e+0[†]	7.388e+0
	5	3.030e+1 [†]	3.036e+1 [†]	3.150e+1 [†]	3.113e+1 [†]	2.872e+1 [†]	3.160e+1 [†]	3.140e+1 [†]	3.148e+1 [†]	3.157e+1 [†]	3.163e+1
	8	2.028e+2 [†]	1.912e+2 [†]	2.491e+2 [†]	2.545e+2 [†]	2.236e+2 [†]	2.556e+2 [†]	2.542e+2 [†]	2.546e+2 [†]	2.553e+2 [†]	2.558e+2
	10	8.226e+2 [†]	5.120e+2 [†]	1.006e+3 [†]	1.019e+3 [†]	9.682e+2 [†]	1.023e+3 [†]	1.019e+3 [†]	1.020e+3 [†]	1.023e+3 [†]	1.024e+3
	15	1.813e+4 [†]	1.638e+4 [†]	3.095e+4 [†]	3.272e+4 [†]	3.024e+4 [†]	3.233e+4 [†]	3.267e+4 [†]	3.153e+4 [†]	3.275e+4 [†]	3.276e+4
WFG8	3	6.989e+0 [†]	7.096e+0 [‡]	7.062e+0	7.069e+0	6.623e+0 [†]	7.124e+0 [‡]	7.082e+0	7.073e+0	7.185e+0[‡]	7.082e+0
	5	2.870e+1 [†]	2.958e+1 [†]	3.072e+1 [†]	2.988e+1 [†]	2.775e+1 [†]	3.061e+1 [†]	3.042e+1 [†]	3.043e+1 [†]	3.081e+1 [†]	3.115e+1
	8	1.425e+2 [†]	1.277e+2 [†]	2.477e+2 [†]	2.431e+2 [†]	2.230e+2 [†]	2.519e+2 [†]	2.468e+2 [†]	2.473e+2 [†]	2.515e+2 [†]	2.542e+2
	10	5.725e+2 [†]	4.530e+2 [†]	9.986e+2 [†]	9.773e+2 [†]	9.496e+2 [†]	1.015e+3 [†]	9.980e+2 [†]	9.989e+2 [†]	1.016e+3 [†]	1.021e+3
	15	1.887e+4 [†]	1.476e+4 [†]	3.075e+4 [†]	3.235e+4 [†]	2.997e+4 [†]	3.022e+4 [†]	3.250e+4 [†]	2.827e+4 [†]	3.264e+4 [†]	3.266e+4
WFG9	3	6.749e+0 [†]	6.796e+0 [†]	6.869e+0 [†]	7.002e+0	6.725e+0 [†]	7.032e+0	6.971e+0	6.985e+0	7.017e+0	7.014e+0
	5	2.885e+1	2.799e+1 [†]	2.900e+1 [†]	2.884e+1 [†]	2.730e+1 [†]	2.981e+1	2.923e+1 [†]	2.935e+1	2.960e+1	2.928e+1
	8	2.021e+2 [†]	2.322e+2 [†]	2.304e+2 [†]	2.318e+2 [†]	2.046e+2 [†]	2.434e+2[‡]	2.317e+2 [†]	2.346e+2	2.351e+2	2.330e+2
	10	7.080e+2 [†]	5.795e+2 [†]	9.200e+2 [†]	9.264e+2 [†]	8.529e+2 [†]	9.826e+2[‡]	9.350e+2 [†]	9.360e+2 [†]	9.410e+2	9.376e+2
	15	1.685e+4 [†]	1.500e+4 [†]	2.884e+4 [†]	2.937e+4 [†]	2.731e+4 [†]	3.069e+4[‡]	2.911e+4 [†]	2.931e+4	2.884e+4 [†]	2.957e+4

According to Wilcoxon's rank sum test, [†] and [‡] indicates whether the corresponding algorithm is significantly worse or better than MOEA/AD respectively.

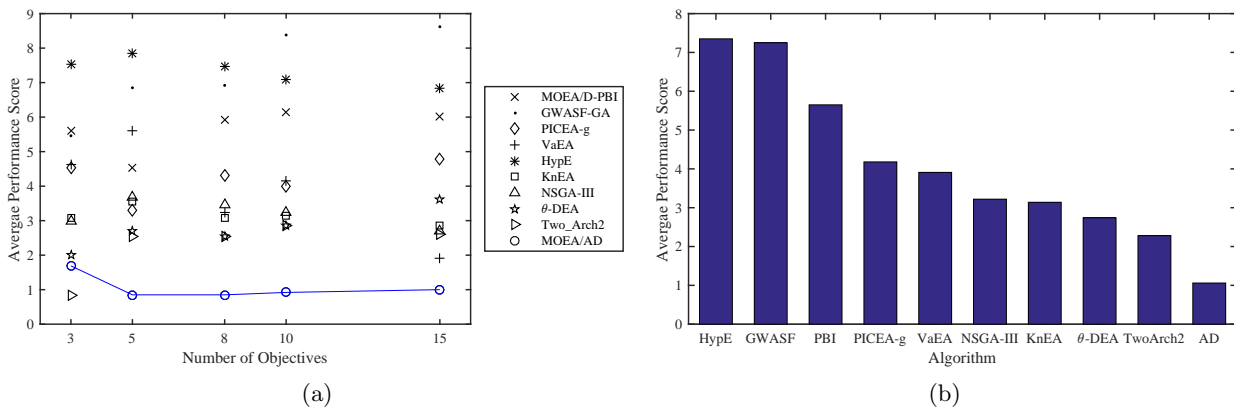


Figure 4: (a) Average performance scores on different number of objectives over DTLZ and WFG problem instances. (b) Average performance scores over all DTLZ and WFG problem instances.

maintaining two complementary populations, the overall performance of our proposed MOEA/AD remains the best on the WFG instances.

To have a better overall comparison among different algorithms, we employ the performance score proposed in [18] to rank the performance of different algorithms over different types of problem instances. Given K algorithms, i.e. A_1, \dots, A_K , the performance score of an algorithm $A_i, i \in$

Table 4: Comparison Results of MOEA/AD and 9 Peer Algorithms on DTLZ⁻¹ Problem Instances.

Problem	m	IPBI	GWASF	PICEA-g	VaEA	HypE	KnEA	NSGA-III	θ -DEA	TwoArch2	MOEA/AD
DTLZ1 ⁻¹	3	5.048e+0 [†]	5.357e+0 [†]	3.840e+0 [†]	5.317e+0 [†]	5.344e+0 [†]	4.659e+0 [†]	5.318e+0 [†]	5.257e+0 [†]	5.361e+0 [†]	5.394e+0
	5	8.696e+0 [†]	1.021e+1 [†]	5.550e+0 [†]	1.016e+1 [†]	1.016e+1 [†]	7.865e+0 [†]	8.780e+0 [†]	6.791e+0 [†]	9.926e+0 [†]	1.088e+1
	8	1.765e+1 [†]	8.880e+0 [†]	6.900e+0 [†]	1.883e+1 [†]	1.838e+1 [†]	6.773e+0 [†]	6.640e+0 [†]	2.538e+0 [†]	1.359e+1 [†]	1.949e+1
	10	2.600e+1 [†]	1.119e+1 [†]	8.024e+0 [†]	2.815e+1 [†]	2.305e+1 [†]	1.183e+1 [†]	7.692e+0 [†]	2.497e+0 [†]	1.586e+1 [†]	2.946e+1
	15	4.124e+1	6.375e+0 [†]	6.842e+0 [†]	3.918e+1 [†]	1.652e+1 [†]	1.079e+1 [†]	6.047e+0 [†]	2.508e+0 [†]	1.905e+1 [†]	4.125e+1
DTLZ2 ⁻¹	3	6.725e+0[‡]	6.622e+0 [†]	5.044e+0 [†]	6.611e+0 [†]	5.592e+0 [†]	6.523e+0 [†]	6.628e+0 [†]	6.563e+0 [†]	6.708e+0 [†]	6.689e+0
	5	1.773e+1	1.356e+1 [†]	1.052e+1 [†]	1.666e+1 [†]	8.986e+0 [†]	1.371e+1 [†]	1.626e+1 [†]	1.522e+1 [†]	1.759e+1 [†]	1.774e+1
	8	4.509e+1 [†]	2.981e+1 [†]	1.805e+1 [†]	4.212e+1 [†]	2.078e+1 [†]	2.285e+1 [†]	2.409e+1 [†]	1.858e+1 [†]	4.569e+1 [†]	4.941e+1
	10	7.820e+1 [†]	3.308e+1 [†]	2.058e+1 [†]	7.809e+1 [†]	2.938e+1 [†]	4.566e+1 [†]	3.705e+1 [†]	1.751e+1 [†]	8.405e+1 [†]	9.045e+1
	15	9.507e+1 [†]	4.900e+1 [†]	2.131e+1 [†]	1.408e+2 [†]	5.276e+1 [†]	5.544e+1 [†]	3.028e+1 [†]	2.045e+1 [†]	8.979e+1 [†]	1.491e+2
DTLZ3 ⁻¹	3	6.359e+0[‡]	6.266e+0 [†]	5.005e+0 [†]	6.251e+0 [†]	5.918e+0 [†]	6.139e+0 [†]	6.297e+0 [†]	6.234e+0 [†]	6.340e+0 [†]	6.328e+0
	5	1.636e+1	1.261e+1 [†]	1.024e+1 [†]	1.518e+1 [†]	1.055e+1 [†]	1.171e+1 [†]	1.438e+1 [†]	1.385e+1 [†]	1.613e+1 [†]	1.636e+1
	8	4.095e+1 [†]	2.725e+1 [†]	1.674e+1 [†]	3.732e+1 [†]	2.353e+1 [†]	1.232e+1 [†]	2.075e+1 [†]	1.501e+1 [†]	4.009e+1 [†]	4.415e+1
	10	7.043e+1 [†]	2.844e+1 [†]	2.262e+1 [†]	6.802e+1 [†]	3.698e+1 [†]	2.186e+1 [†]	3.086e+1 [†]	1.386e+1 [†]	7.189e+1 [†]	8.018e+1
	15	8.678e+1 [†]	4.581e+1 [†]	2.245e+1 [†]	1.248e+2 [†]	3.980e+1 [†]	3.594e+1 [†]	3.176e+1 [†]	1.778e+1 [†]	8.691e+1 [†]	1.313e+2
DTLZ4 ⁻¹	3	6.578e+0 [†]	6.623e+0 [†]	4.255e+0 [†]	6.632e+0 [†]	5.316e+0 [†]	6.538e+0 [†]	6.669e+0 [†]	6.621e+0 [†]	6.706e+0[‡]	6.694e+0
	5	1.742e+1 [†]	1.355e+1 [†]	8.304e+0 [†]	1.680e+1 [†]	8.840e+0 [†]	1.397e+1 [†]	1.651e+1 [†]	1.503e+1 [†]	1.761e+1 [†]	1.777e+1
	8	4.339e+1 [†]	3.225e+1 [†]	1.218e+1 [†]	4.255e+1 [†]	1.675e+1 [†]	2.280e+1 [†]	2.872e+1 [†]	1.197e+1 [†]	4.578e+1 [†]	4.856e+1
	10	7.816e+1 [†]	5.378e+1 [†]	1.911e+1 [†]	7.831e+1 [†]	1.995e+1 [†]	4.790e+1 [†]	4.238e+1 [†]	1.472e+1 [†]	8.423e+1 [†]	8.781e+1
	15	8.953e+1 [†]	4.729e+1 [†]	2.226e+1 [†]	1.384e+2 [†]	3.040e+1 [†]	5.869e+1 [†]	1.468e+1 [†]	3.091e+1 [†]	9.467e+1 [†]	1.460e+2

According to Wilcoxon's rank sum test, [†] and [‡] indicates whether the corresponding algorithm is significantly worse or better than MOEA/AD respectively.

$\{1, \dots, K\}$, is defined as

$$P(A_i) = \sum_{j=1, j \neq i}^K \delta_{i,j}, \quad (13)$$

where $\delta_{i,j} = 1$ if A_j is significant better than A_i according to the Wilcoxon's rank sum test; otherwise, $\delta_{i,j} = 0$. In other words, the performance score of an algorithm counts the number of competitors that outperform it on a given problem instance. Thus, the smaller performance score, the better an algorithm performs. The average performance scores of different algorithms on DTLZ and WFG problem instances are shown in Fig. 4. From Fig. 4(a), we find that MOEA/AD is the best algorithm on problems with more than 3 objectives and its better scores are of statistical significance. Two_Arch2 shows the best performance on the 3-objective cases, but its performance significantly degenerates with the dimensionality. By aggregating the average performance scores on all problem instances, Fig. 4(b) demonstrates the comparisons on all DTLZ and WFG problem instances. Similar to the previous observation, followed by θ -DEA and Two_Arch2, our proposed MOEA/AD obtains the best overall performance.

5.2 Comparisons on DTLZ⁻¹ and WFG⁻¹ Problem Instances

The comparison results on the DTLZ⁻¹ problem instances are given in Table 4. Similar to the observations in Table 2, MOEA/AD is the best algorithm which wins on almost all comparisons (150 out of 153) except for the 3-objective DTLZ1⁻¹, DTLZ3⁻¹ and DTLZ4⁻¹ instances. In particular, MOEA/D-IPBI shows better performance than MOEA/AD on the 3-objective DTLZ2⁻¹ and DTLZ3⁻¹ instances, while Two_Arch2 outperforms MOEA/AD on the 3-objective DTLZ2⁻¹ to DTLZ4⁻¹ instances. The inferior performance of MOEA/AD might be partially caused by the disturbance from its normalization procedure. As discussed in [65], uniformly sampled weight vectors upon the simplex tend to guide the population towards the boundaries of a hyperspherical PF (e.g., DTLZ2⁻¹ to DTLZ4⁻¹). This explains the relatively good performance obtained by Two_Arch2 and VaEA which do not rely on a set of fixed weight vectors. However, we also notice that the performance of PICEA-g, HypE and KnEA are not satisfied under this setting. Although Global WASF-GA also uses the nadir point as the reference point in its scalarizing function like MOEA/AD, it fails to obtain comparable performance due to its poor diversity maintenance scheme.

The HV results on WFG⁻¹ problem instances are displayed in Table 5. From Table 5, MOEA/AD achieves the best overall performance on the WFG⁻¹ test suite, where it significantly outperforms its competitor in 369 out of 450 comparisons. WFG1⁻¹ and WFG2⁻¹ have quite complex PF shapes. The best algorithms on WFG1⁻¹ differ with the number of objectives. Global WASF-GA and MOEA/AD show the best HV results on 3- and 5-objective WFG1⁻¹ instances respectively. When the objectives are more than 5, MOEA/D-IPBI, PICEA-g, VaEA and KnEA become the

Table 5: Comparison Results of MOEA/AD and 9 Peer Algorithms on WFG⁻¹ Problem Instances.

Problem	m	IPBI	GWASF	PICEA-g	VaEA	HypE	KnEA	NSGA-III	θ -DEA	TwoArch2	MOEA/AD
WFG1 ⁻¹	3	3.704e+0 [†]	4.219e+0[‡]	3.370e+0 [†]	3.151e+0 [†]	2.353e+0 [†]	4.154e+0 [‡]	3.041e+0 [†]	3.007e+0 [†]	3.886e+0	3.892e+0
	5	5.402e+0 [†]	6.713e+0	5.652e+0 [†]	5.121e+0 [†]	3.014e+0 [†]	5.915e+0 [†]	3.537e+0 [†]	5.067e+0 [†]	3.110e+0 [†]	6.727e+0
	8	7.430e+0 [†]	2.832e+0 [†]	7.278e+0 [‡]	6.675e+0 [‡]	2.944e+0 [†]	7.614e+0[‡]	3.479e+0 [†]	4.742e+0 [‡]	2.972e+0 [†]	3.920e+0
	10	1.011e+1 [†]	3.481e+0 [†]	1.085e+1[‡]	8.997e+0 [‡]	2.957e+0 [†]	1.071e+1 [†]	3.602e+0	5.362e+0 [‡]	2.946e+0 [†]	3.735e+0
	15	1.434e+1[†]	1.849e+0 [†]	1.091e+1 [†]	1.097e+1 [†]	4.132e+0 [†]	8.360e+0 [†]	3.397e+0 [†]	3.745e+0 [†]	2.993e+0 [†]	4.693e+0
WFG2 ⁻¹	3	5.987e+0 [†]	6.084e+0 [†]	4.673e+0 [†]	6.091e+0 [†]	5.878e+0 [†]	5.754e+0 [†]	6.104e+0 [†]	6.108e+0 [†]	6.069e+0 [†]	6.134e+0
	5	9.557e+0 [†]	1.016e+1 [†]	5.210e+0 [†]	1.099e+1 [†]	8.914e+0 [†]	8.839e+0 [†]	9.498e+0 [†]	1.031e+1 [†]	8.272e+0 [†]	1.117e+1
	8	1.530e+1 [†]	6.643e+0 [†]	4.397e+0 [†]	1.799e+1[†]	9.955e+0 [†]	1.125e+1 [†]	8.135e+0 [†]	9.735e+0 [†]	7.879e+0 [†]	1.746e+1
	10	1.908e+1 [†]	7.388e+0 [†]	4.519e+0 [†]	2.390e+1 [†]	1.241e+1 [†]	1.569e+1 [†]	8.431e+0 [†]	9.237e+0 [†]	7.647e+0 [†]	2.447e+1
	15	2.794e+1 [†]	3.472e+0 [†]	3.366e+0 [†]	3.124e+1 [†]	1.760e+1 [†]	1.374e+1 [†]	8.035e+0 [†]	6.240e+0 [†]	7.501e+0 [†]	3.587e+1
WFG3 ⁻¹	3	4.779e+0 [†]	5.445e+0	3.695e+0 [†]	5.370e+0 [†]	4.373e+0 [†]	4.430e+0 [†]	5.283e+0 [†]	5.327e+0 [†]	5.447e+0	5.447e+0
	5	7.877e+0 [†]	1.043e+1 [†]	4.872e+0 [†]	1.051e+1 [†]	6.368e+0 [†]	7.286e+0 [†]	8.213e+0 [†]	7.307e+0 [†]	1.005e+1 [†]	1.104e+1
	8	1.124e+1 [†]	8.709e+0 [†]	4.670e+0 [†]	1.959e+1 [†]	7.962e+0 [†]	1.027e+1 [†]	7.321e+0 [†]	3.576e+0 [†]	1.144e+1 [†]	1.986e+1
	10	1.469e+1 [†]	1.076e+1 [†]	5.122e+0 [†]	2.899e+1 [†]	1.027e+1 [†]	1.597e+1 [†]	8.023e+0 [†]	2.679e+0 [†]	1.313e+1 [†]	2.983e+1
	15	1.960e+1 [†]	5.816e+0 [†]	3.983e+0 [†]	3.957e+1 [†]	1.232e+1 [†]	1.640e+1 [†]	6.675e+0 [†]	8.462e+1 [†]	1.963e+1 [†]	4.094e+1
WFG4 ⁻¹	3	6.694e+0 [‡]	6.616e+0 [†]	5.692e+0 [†]	6.474e+0 [†]	5.746e+0 [†]	6.016e+0 [†]	6.390e+0 [†]	6.466e+0 [†]	6.675e+0[‡]	6.669e+0
	5	1.723e+1 [†]	1.362e+1 [†]	1.392e+1 [†]	1.592e+1 [†]	1.081e+1 [†]	8.779e+0 [†]	1.477e+1 [†]	1.500e+1 [†]	1.761e+1	1.670e+1
	8	4.044e+1 [†]	2.959e+1 [†]	2.182e+1 [†]	4.152e+1 [†]	1.669e+1 [†]	1.542e+1 [†]	2.158e+1 [†]	1.943e+1 [†]	4.518e+1 [†]	4.687e+1
	10	6.781e+1 [†]	3.521e+1 [†]	3.171e+1 [†]	7.704e+1 [†]	2.403e+1 [†]	2.429e+1 [†]	3.532e+1 [†]	1.417e+1 [†]	7.737e+1 [†]	8.534e+1
	15	8.277e+1 [†]	5.149e+1 [†]	1.333e+1 [†]	1.444e+2 [†]	3.998e+1 [†]	2.686e+1 [†]	3.787e+1 [†]	3.637e+0 [†]	5.919e+1 [†]	1.486e+2
WFG5 ⁻¹	3	6.683e+0 [‡]	6.605e+0 [†]	5.708e+0 [†]	6.487e+0 [†]	5.414e+0 [†]	6.105e+0 [†]	6.444e+0 [†]	6.515e+0 [†]	6.686e+0[‡]	6.665e+0
	5	1.723e+1 [†]	1.373e+1 [†]	1.313e+1 [†]	1.648e+1 [†]	1.075e+1 [†]	8.647e+0 [†]	1.554e+1 [†]	1.496e+1 [†]	1.737e+1 [†]	1.769e+1
	8	4.065e+1 [†]	3.111e+1 [†]	2.486e+1 [†]	4.026e+1 [†]	1.852e+1 [†]	1.564e+1 [†]	2.444e+1 [†]	1.768e+1 [†]	4.329e+1 [†]	4.771e+1
	10	6.840e+1 [†]	3.004e+1 [†]	3.780e+1 [†]	7.694e+1 [†]	2.641e+1 [†]	2.285e+1 [†]	3.573e+1 [†]	1.111e+1 [†]	7.438e+1 [†]	8.627e+1
	15	8.410e+1 [†]	4.579e+1 [†]	6.327e+1 [†]	1.412e+2 [†]	4.360e+1 [†]	2.790e+1 [†]	3.888e+1 [†]	5.382e+0 [†]	6.110e+1 [†]	1.460e+2
WFG6 ⁻¹	3	6.693e+0 [‡]	6.619e+0 [†]	5.775e+0 [†]	6.564e+0 [†]	5.110e+0 [†]	6.317e+0 [†]	6.539e+0 [†]	6.548e+0 [†]	6.703e+0[‡]	6.676e+0
	5	1.723e+1 [†]	1.357e+1 [†]	1.372e+1 [†]	1.681e+1 [†]	9.565e+0 [†]	9.297e+0 [†]	1.589e+1 [†]	1.506e+1 [†]	1.753e+1 [†]	1.771e+1
	8	4.049e+1 [†]	3.076e+1 [†]	2.783e+1 [†]	3.954e+1 [†]	1.705e+1 [†]	1.561e+1 [†]	2.435e+1 [†]	1.628e+1 [†]	4.460e+1 [†]	4.810e+1
	10	6.792e+1 [†]	3.684e+1 [†]	4.418e+1 [†]	7.574e+1 [†]	2.455e+1 [†]	2.014e+1 [†]	3.586e+1 [†]	9.602e+0 [†]	7.944e+1 [†]	8.714e+1
	15	8.136e+1 [†]	4.105e+1 [†]	5.323e+1 [†]	1.383e+2 [†]	3.667e+1 [†]	2.072e+1 [†]	4.102e+1 [†]	6.963e+0 [†]	8.900e+1 [†]	1.460e+2
WFG7 ⁻¹	3	6.694e+0 [‡]	6.610e+0 [†]	5.965e+0 [†]	6.519e+0 [†]	5.814e+0 [†]	5.748e+0 [†]	6.455e+0 [†]	6.537e+0 [†]	6.706e+0[‡]	6.665e+0
	5	1.723e+1 [†]	1.357e+1 [†]	1.418e+1 [†]	1.648e+1 [†]	1.000e+1 [†]	8.338e+0 [†]	1.537e+1 [†]	1.501e+1 [†]	1.755e+1 [†]	1.765e+1
	8	4.046e+1 [†]	3.132e+1 [†]	2.392e+1 [†]	3.983e+1 [†]	1.658e+1 [†]	1.492e+1 [†]	2.272e+1 [†]	1.763e+1 [†]	4.395e+1 [†]	4.690e+1
	10	6.787e+1 [†]	4.803e+1 [†]	3.421e+1 [†]	7.558e+1 [†]	2.308e+1 [†]	2.199e+1 [†]	3.361e+1 [†]	1.236e+1 [†]	7.549e+1 [†]	8.515e+1
	15	8.381e+1 [†]	3.392e+1 [†]	2.380e+1 [†]	1.408e+2 [†]	4.449e+1 [†]	1.739e+1 [†]	3.384e+1 [†]	4.568e+0 [†]	8.796e+1 [†]	1.475e+2
WFG8 ⁻¹	3	6.693e+0[‡]	6.619e+0 [†]	6.073e+0 [†]	6.554e+0 [†]	6.048e+0 [†]	6.449e+0 [†]	6.566e+0 [†]	6.550e+0 [†]	6.690e+0 [†]	6.683e+0
	5	1.722e+1 [†]	1.355e+1 [†]	1.461e+1 [†]	1.700e+1 [†]	9.001e+0 [†]	1.197e+1 [†]	1.614e+1 [†]	1.485e+1 [†]	1.749e+1 [†]	1.774e+1
	8	4.054e+1 [†]	3.160e+1 [†]	3.148e+1 [†]	4.329e+1 [†]	1.759e+1 [†]	2.354e+1 [†]	2.548e+1 [†]	1.746e+1 [†]	4.521e+1 [†]	4.799e+1
	10	6.805e+1 [†]	3.128e+1 [†]	5.119e+1 [†]	7.992e+1 [†]	2.518e+1 [†]	5.337e+1 [†]	3.799e+1 [†]	1.205e+1 [†]	8.332e+1 [†]	8.708e+1
	15	8.302e+1 [†]	4.373e+1 [†]	5.093e+1 [†]	1.529e+2[‡]	3.877e+1 [†]	6.124e+1 [†]	4.135e+1 [†]	6.750e+0 [†]	1.275e+2 [†]	1.464e+2
WFG9 ⁻¹	3	6.665e+0 [‡]	6.565e+0 [†]	6.332e+0 [†]	6.520e+0 [†]	5.345e+0 [†]	6.305e+0 [†]	6.498e+0 [†]	6.529e+0 [†]	6.675e+0[‡]	6.634e+0
	5	1.720e+1 [†]	1.382e+1 [†]	1.535e+1 [†]	1.673e+1 [†]	1.089e+1 [†]	1.429e+1 [†]	1.597e+1 [†]	1.509e+1 [†]	1.741e+1 [†]	1.748e+1
	8	4.060e+1 [†]	3.124e+1 [†]	3.145e+1 [†]	4.230e+1 [†]	1.971e+1 [†]	1.920e+1 [†]	2.644e+1 [†]	1.322e+1 [†]	4.404e+1 [†]	4.692e+1
	10	6.905e+1 [†]	4.819e+1 [†]	5.044e+1 [†]	7.767e+1 [†]	2.453e+1 [†]	3.322e+1 [†]	4.016e+1 [†]	8.968e+0 [†]	7.848e+1 [†]	8.549e+1
	15	8.989e+1 [†]	4.867e+1 [†]	6.333e+1 [†]	1.432e+2	4.166e+1 [†]	4.476e+1 [†]	5.153e+1 [†]	7.383e+0 [†]	1.175e+2 [†]	1.444e+2

According to Wilcoxon's rank sum test, [†] and [‡] indicates whether the corresponding algorithm is significantly worse or better than MOEA/AD respectively.

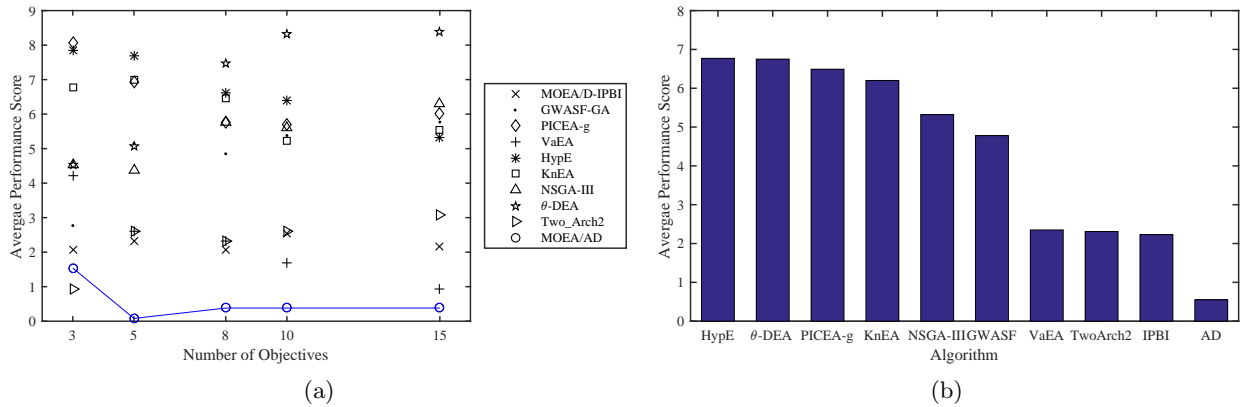


Figure 5: (a) Average performance scores on different number of objectives over DTLZ⁻¹ and WFG⁻¹ problem instances. (b) Average performance scores over all DTLZ⁻¹ and WFG⁻¹ problem instances.

best four algorithms, three of which do not use fixed weight vectors to guide the search. In contrast, MOEA/AD is the best algorithm on all WFG2⁻¹ instances. Even though VaEA has a slightly larger mean HV metric value on 8-objective WFG2⁻¹, MOEA/AD is shown to be significantly better in all 45 comparisons according to Wilcoxon's rank sum test. The PFs of WFG3⁻¹ instances are hyperplanes, which are perfect for decomposition-based algorithms using the nadir point. MOEA/AD remains being the best algorithm on all 5 problem instances, while MOEA/D-IPBI does not perform

Algorithm 6: MatingSelectionV2($S_c, S_d, i, M, R, C, W, B$)

```
1 pop ← PopSelection( $S_c, S_d, i, M, W$ );
2 if rand <  $\delta$  then
3    $S_p \leftarrow \emptyset$ ;
4   if pop == 1 then
5     for  $j \leftarrow 1$  to  $T$  do
6        $S_p \leftarrow S_p \cup \{\mathbf{x}_d^{B[i][j]}\}$ ;
7        $\mathbf{x}^r \leftarrow$  Randomly select a solution from  $S_p$ ;
8        $\bar{S} \leftarrow \{\mathbf{x}_d^i, \mathbf{x}^r\}$ ;
9   else
10    for  $j \leftarrow 1$  to  $T$  do
11       $S_p \leftarrow S_p \cup \{\mathbf{x}_c^{B[M[i]][j]}\}$ ;
12       $\mathbf{x}^r \leftarrow$  Randomly select a solution from  $S_p$ ;
13       $\bar{S} \leftarrow \{\mathbf{x}_c^{M[i]}, \mathbf{x}^r\}$ ;
14 else
15   if pop == 1 then
16      $\mathbf{x}^r \leftarrow$  Randomly select a solution from  $S_d$ ;
17      $\bar{S} \leftarrow \{\mathbf{x}_d^i, \mathbf{x}^r\}$ ;
18   else
19      $\mathbf{x}^r \leftarrow$  Randomly select a solution from  $S_c$ ;
20      $\bar{S} \leftarrow \{\mathbf{x}_c^{M[i]}, \mathbf{x}^r\}$ ;
21 return  $\bar{S}$ 
```

as good as expected. It is also worth noting that Two_Arch2 never beats MOEA/AD on WFG1⁻¹ to WFG3⁻¹ instances. The PFs of WFG4⁻¹ to WFG9⁻¹ are hyperspheres centered at the nadir point. MOEA/AD is significantly better than the other algorithms on all 5- to 15-objective WFG4⁻¹ to WFG9⁻¹ instances except that it is outperformed by Two_Arch2 and VaEA on 5-objective WFG4⁻¹ and 15-objective WFG8⁻¹ respectively. The reason why MOEA/AD outperforms the other algorithms, including Two_Arch2, is not simply due to the co-evolving populations but mainly because of the adversarial search directions and the well constructed collaboration for reproduction. Similar to the situation on DTLZ⁻¹ test suite, Two_Arch2 and MOEA/D-IPBI are the best two algorithms on 3-objective WFG4⁻¹ to WFG9⁻¹ instances.

We calculate the average performance scores of different algorithms on DTLZ⁻¹ and WFG⁻¹ test suites and display the results in Fig. 5. As shown in Fig. 5(b), MOEA/AD, whose average performance score is four times smaller than the runner-up, remains the best among all test algorithms. It is worth noting that the final ranking of MOEA/D and Global WASF-GA increase dramatically compared with Fig. 4 due to the use of nadir point. However, the ranking of θ -DEA, which adopts fixed weight vectors starting from the ideal point, drops significantly. More specifically, from Fig. 5(a), MOEA/AD achieves the best average performance scores on problems with more than three objectives and obtains the second best results problems with 3 and 15 objectives. Following MOEA/AD, the performance of Two_Arch2 degenerates when the number of objectives increases, whereas, the performance of VaEA is improved with the number of objectives.

5.3 Performance Comparisons with Three Variants

In our proposed MOEA/AD, there are two major aspects that contribute to the complementary effect of two co-evolving populations: one is the use of two scalarizing functions which results in the adversarial search directions; the other is the sophisticated mating selection process. The effectiveness of the prior aspect has been validated in the comparisons with the MOEA/D variants

Table 6: Comparison Results of MOEA/AD and its Three Variants on DTLZ Problem Instances.

Problem	m	AD- <i>v</i> 1	AD- <i>v</i> 2	AD- <i>v</i> 3	AD
DTLZ1	3	7.785e+0 [†]	7.785e+0 [†]	7.777e+0 [†]	7.787e+0
	5	3.197e+1 [†]	3.196e+1 [†]	3.191e+1 [†]	3.197e+1
	8	2.560e+2 [†]	2.491e+2 [†]	2.499e+2 [†]	2.560e+2
	10	1.008e+3 [†]	9.767e+2 [†]	1.006e+3 [†]	1.024e+3
	15	3.055e+4 [†]	3.186e+4 [†]	3.098e+4 [†]	3.270e+4
DTLZ2	3	7.412e+0	7.412e+0	7.411e+0 [†]	7.412e+0
	5	3.170e+1	3.170e+1	3.170e+1 [†]	3.170e+1
	8	2.558e+2 [†]	2.558e+2 [†]	2.558e+2 [†]	2.558e+2
	10	1.024e+3 [†]	1.024e+3 [†]	1.024e+3	1.024e+3
	15	3.276e+4	3.276e+4	3.276e+4	3.276e+4
DTLZ3	3	7.405e+0	7.239e+0	7.405e+0	7.403e+0
	5	3.097e+1 [†]	2.877e+1 [†]	3.092e+1 [†]	3.169e+1
	8	2.125e+2 [†]	2.330e+2 [†]	2.058e+2 [†]	2.558e+2
	10	8.783e+2 [†]	8.356e+2 [†]	6.739e+2 [†]	1.024e+3
	15	2.761e+4 [†]	2.574e+4 [†]	2.681e+4 [†]	3.276e+4
DTLZ4	3	7.410e+0 [†]	7.411e+0	7.410e+0 [†]	7.412e+0
	5	3.169e+1	3.169e+1	3.169e+1	3.169e+1
	8	2.558e+2	2.558e+2	2.558e+2	2.558e+2
	10	1.024e+3	1.024e+3	1.024e+3	1.024e+3
	15	3.276e+4	3.276e+4 [†]	3.276e+4	3.276e+4

According to Wilcoxon’s rank sum test, [†] and [‡] indicates whether the corresponding algorithm is significantly worse or better than MOEA/AD respectively.

with a single scalarizing function. To further investigate the effectiveness of the sophisticated mating selection process, we design the following three variants to validate its three major components, i.e., the pairing step, the mating selection step and the principal parent selection.

- MOEA/AD-*v*1: it replaces the two-level stable matching in line 13 of Algorithm 1 with random matching. In particular, M is set as a random permutation among 1 to N and $R[i] = 1$ for all $i \in \{1, \dots, N\}$.
- MOEA/AD-*v*2: it does not consider the collaboration between S_d and S_c in the mating selection step. In particular, it randomly selects the mating parents from S_d and S_c according to the principal parent. The pseudo code is given in Algorithm 6.
- MOEA/AD-*v*3: it only considers one criteria, i.e., subproblem’s relative improvement, to select the principal parent solution. In short, line 6-11 of Algorithm 4 are replaced by $pop \leftarrow$ Randomly select from $\{1, 2\}$.

The comparison results between MOEA/AD and its three variants are presented in Table 6. We find that our proposed MOEA/AD is still the best candidate where it obtains the best mean HV values on 16 out of 20 problem instances. In particular, its better HV values are with statistical significance on almost all DTLZ1 and DTLZ3 instances. Although MOEA/AD is outperformed by its variants on some instances, the differences to the best results are quite small. We have the following three assertions from the comparison results.

- The stable matching procedure divides solutions of two populations into different pairs according to their working regions of the PF. It facilitates the mating selection process and help spread the search efforts along the while PF. In the meanwhile, the solution pair also provides some addition information on whether the paired solutions work on the similar regions.
- The collaboration between two populations help strengthen their complementary behaviors, i.e., one is diversity oriented and the other is convergence oriented.

- The three criteria together help to select a promising principal parent solution from a matching pair, which makes the reproduction more efficient.

6 Conclusion

In this paper, we have proposed MOEA/AD, a many-objective optimization algorithm based on adversarial decomposition. Specifically, it maintains two co-evolving populations simultaneously. Due to the use of different scalarizing functions, these two co-evolving populations have adversarial search directions which finally results in their complementary behaviors. In particular, one is convergence oriented and the other is diversity oriented. The collaboration between these two populations is implemented by a restricted mating selection scheme. At first, solutions from the two populations are stably matched into different one-one solution pairs according to their working regions. During the mating selection procedure, each matching pair can at most contribute one mating parent for offspring generation. By doing this, we can expect to avoid allocating redundant computational resources to the same region of the PF. By comparing the performance with nine state-of-the-art many-objective optimization algorithms on 130 problem instances, we have witnessed the effectiveness and competitiveness of MOEA/AD for solving many-objective optimization problems with various characteristics and PF's shapes. As a potential future direction, it is interesting to develop some adaptive methods that determine the scalarizing functions of different subproblems according to the PF's shape. It is also valuable to apply our proposed algorithm to other interesting application problems.

References

- [1] A. Ropponen, R. Ritala, and E. N. Pistikopoulos, "Optimization issues of the broke management system in papermaking," *Computers & Chemical Engineering*, vol. 35, no. 11, pp. 2510–2520, 2011.
- [2] M. G. C. Tapia and C. A. C. Coello, "Applications of multi-objective evolutionary algorithms in economics and finance: A survey," in *CEC'07: Proc. 2007 IEEE Congress on Evolutionary Computation*, Singapore, Sep. 2007, pp. 532–539.
- [3] P. M. Reed and D. Hadka, "Evolving many-objective water management to exploit exascale computing," *Water Resources Research*, vol. 50, no. 10, pp. 8367–8373, 2014.
- [4] K. Deb, *Multi-Objective Optimization Using Evolutionary Algorithms*. New York, NY, USA: John Wiley & Sons, Inc., 2001.
- [5] K. Deb, S. Agrawal, A. Pratap, and T. Meyarivan, "A fast and elitist multiobjective genetic algorithm: NSGA-II," *IEEE Trans. Evolutionary Computation*, vol. 6, no. 2, pp. 182–197, 2002.
- [6] E. Zitzler, M. Laumanns, and L. Thiele, "SPEA2: Improving the strength pareto evolutionary algorithm for multiobjective optimization," in *Evolutionary Methods for Design, Optimisation, and Control*, 2002, pp. 95–100.
- [7] N. Beume, B. Naujoks, and M. T. M. Emmerich, "SMS-EMOA: multiobjective selection based on dominated hypervolume," *European Journal of Operational Research*, vol. 181, no. 3, pp. 1653–1669, 2007.
- [8] K. Li, S. Kwong, R. Wang, J. Cao, and I. J. Rudas, "Multi-objective differential evolution with self-navigation," in *SMC'12: Proc. of the 2012 IEEE International Conference on Systems, Man, and Cybernetics*. Seoul, Korea(South): IEEE, Oct. 2012, pp. 508–513.
- [9] K. Li, S. Kwong, J. Cao, M. Li, J. Zheng, and R. Shen, "Achieving balance between proximity and diversity in multi-objective evolutionary algorithm," *Information Sciences*, vol. 182, no. 1, pp. 220–242, 2012.

- [10] K. Li, S. Kwong, R. Wang, K.-S. Tang, and K.-F. Man, “Learning paradigm based on jumping genes: A general framework for enhancing exploration in evolutionary multiobjective optimization,” *Information Sciences*, vol. 226, pp. 1–22, 2013.
- [11] K. Li and S. Kwong, “A general framework for evolutionary multiobjective optimization via manifold learning,” *Neurocomputing*, vol. 146, pp. 65–74, 2014.
- [12] K. Li, Á. Fialho, S. Kwong, and Q. Zhang, “Adaptive operator selection with bandits for a multiobjective evolutionary algorithm based on decomposition,” *IEEE Transactions on Evolutionary Computation*, vol. 18, no. 1, pp. 114–130, 2014.
- [13] T. Wagner, N. Beume, and B. Naujoks, “Pareto-, aggregation-, and indicator-based methods in many-objective optimization,” in *Evolutionary Multi-Criterion Optimization, 4th International Conference, EMO 2007, Matsushima, Japan, March 5-8, 2007, Proceedings*, 2006, pp. 742–756.
- [14] H. Ishibuchi, N. Tsukamoto, and Y. Nojima, “Evolutionary many-objective optimization: A short review,” in *Proceedings of the IEEE Congress on Evolutionary Computation, CEC 2008, Hong Kong, China, 2008*, pp. 2419–2426.
- [15] B. Li, J. Li, K. Tang, and X. Yao, “Many-objective evolutionary algorithms: A survey,” *ACM Comput. Surv.*, vol. 48, no. 1, pp. 13:1–13:35, 2015.
- [16] K. Deb and H. Jain, “An evolutionary many-objective optimization algorithm using reference-point-based nondominated sorting approach, part I: solving problems with box constraints,” *IEEE Trans. Evolutionary Computation*, vol. 18, no. 4, pp. 577–601, 2014.
- [17] S. F. Adra and P. J. Fleming, “Diversity management in evolutionary many-objective optimization,” *IEEE Trans. Evolutionary Computation*, vol. 15, no. 2, pp. 183–195, 2011.
- [18] J. Bader and E. Zitzler, “Hype: An algorithm for fast hypervolume-based many-objective optimization,” *Evolutionary Computation*, vol. 19, no. 1, pp. 45–76, 2011.
- [19] D. Hadka and P. M. Reed, “Borg: An auto-adaptive many-objective evolutionary computing framework,” *Evolutionary Computation*, vol. 21, no. 2, pp. 231–259, 2013.
- [20] Z. He, G. G. Yen, and J. Zhang, “Fuzzy-based pareto optimality for many-objective evolutionary algorithms,” *IEEE Trans. Evolutionary Computation*, vol. 18, no. 2, pp. 269–285, 2014.
- [21] M. Farina and P. Amato, “A fuzzy definition of ”optimality” for many-criteria optimization problems,” *IEEE Trans. Systems, Man, and Cybernetics, Part A*, vol. 34, no. 3, pp. 315–326, 2004.
- [22] F. di Pierro, S. Khu, and D. A. Savic, “An investigation on preference order ranking scheme for multiobjective evolutionary optimization,” *IEEE Trans. Evolutionary Computation*, vol. 11, no. 1, pp. 17–45, 2007.
- [23] H. Sato, H. E. Aguirre, and K. Tanaka, “Controlling dominance area of solutions and its impact on the performance of moeas,” in *Proceedings of the 4th International Conference on Evolutionary Multi-criterion Optimization*, 2007, pp. 5–20.
- [24] S. Yang, M. Li, X. Liu, and J. Zheng, “A grid-based evolutionary algorithm for many-objective optimization,” *IEEE Trans. Evolutionary Computation*, vol. 17, no. 5, pp. 721–736, 2013.
- [25] C. Zhu, L. Xu, and E. D. Goodman, “Generalization of pareto-optimality for many-objective evolutionary optimization,” *IEEE Trans. Evolutionary Computation*, vol. 20, no. 2, pp. 299–315, 2016.

- [26] X. Zou, Y. Chen, M. Liu, and L. Kang, “A new evolutionary algorithm for solving many-objective optimization problems,” *IEEE Trans. Systems, Man, and Cybernetics, Part B*, vol. 38, no. 5, pp. 1402–1412, 2008.
- [27] E. Zitzler, “Evolutionary algorithms for multiobjective optimization: Methods and applications,” Ph.D. dissertation, Swiss Federal Institute of Technology Zurich, 1999.
- [28] R. Wang, R. C. Purshouse, and P. J. Fleming, “Preference-inspired coevolutionary algorithms for many-objective optimization,” *IEEE Trans. Evolutionary Computation*, vol. 17, no. 4, pp. 474–494, 2013.
- [29] N. Beume, C. M. Fonseca, M. López-Ibáñez, L. Paquete, and J. Vahrenhold, “On the complexity of computing the hypervolume indicator,” *IEEE Trans. Evolutionary Computation*, vol. 13, no. 5, pp. 1075–1082, 2009.
- [30] K. Bringmann and T. Friedrich, “Approximating the volume of unions and intersections of high-dimensional geometric objects,” *Comput. Geom.*, vol. 43, no. 6-7, pp. 601–610, 2010.
- [31] R. L. While, L. Bradstreet, and L. Barone, “A fast way of calculating exact hypervolumes,” *IEEE Trans. Evolutionary Computation*, vol. 16, no. 1, pp. 86–95, 2012.
- [32] X. Zhang, Y. Tian, R. Cheng, and Y. Jin, “An efficient approach to nondominated sorting for evolutionary multiobjective optimization,” *IEEE Transactions on Evolutionary Computation*, vol. 19, no. 2, pp. 201–213, Apr. 2015.
- [33] Y. Zhou, Z. Chen, and J. Zhang, “Ranking vectors by means of the dominance degree matrix,” *IEEE Trans. Evolutionary Computation*, vol. 21, no. 1, pp. 34–51, 2017.
- [34] P. Gustavsson and A. Syberfeldt, “A new algorithm using the non-dominated tree to improve non-dominated sorting,” *Evolutionary Computation*, 2017, accepted for publication.
- [35] K. Li, K. Deb, Q. Zhang, and Q. Zhang, “Efficient non-domination level update method for steady-state evolutionary multiobjective optimization,” *IEEE Trans. Cybernetics*, 2016, accepted for publication.
- [36] H. Ishibuchi, Y. Sakane, N. Tsukamoto, and Y. Nojima, “Evolutionary many-objective optimization by NSGA-II and MOEA/D with large populations,” in *SMC’09: Proc. of the 2009 IEEE International Conference on Systems, Man and Cybernetics*, 2009, pp. 1758–1763.
- [37] H. Ishibuchi, N. Akedo, and Y. Nojima, “Behavior of multiobjective evolutionary algorithms on many-objective knapsack problems,” *IEEE Trans. Evolutionary Computation*, vol. 19, no. 2, pp. 264–283, 2015.
- [38] H. Ishibuchi, Y. Setoguchi, H. Masuda, and Y. Nojima, “How to compare many-objective algorithms under different settings of population and archive sizes,” in *IEEE Congress on Evolutionary Computation, CEC 2016, Vancouver, BC, Canada*, 2016, pp. 1149–1156.
- [39] A. Zhou and Q. Zhang, “Are all the subproblems equally important? resource allocation in decomposition-based multiobjective evolutionary algorithms,” *IEEE Trans. Evolutionary Computation*, vol. 20, no. 1, pp. 52–64, 2016.
- [40] K. Li, S. Kwong, Q. Zhang, and K. Deb, “Interrelationship-based selection for decomposition multiobjective optimization,” *IEEE Trans. Cybernetics*, vol. 45, no. 10, pp. 2076–2088, 2015.
- [41] Y. Yuan, H. Xu, B. Wang, B. Zhang, and X. Yao, “Balancing convergence and diversity in decomposition-based many-objective optimizers,” *IEEE Trans. Evolutionary Computation*, vol. 20, no. 2, pp. 180–198, 2016.

- [42] M. Asafuddoula, T. Ray, and R. A. Sarker, “A decomposition-based evolutionary algorithm for many objective optimization,” *IEEE Trans. Evolutionary Computation*, vol. 19, no. 3, pp. 445–460, 2015.
- [43] Z. He and G. Yen, “Many-objective evolutionary algorithms based on coordinated selection strategy,” *IEEE Trans. on Evolutionary Computation*, 2016, accepted for publication.
- [44] K. Li, K. Deb, Q. Zhang, and S. Kwong, “An evolutionary many-objective optimization algorithm based on dominance and decomposition,” *IEEE Trans. Evolutionary Computation*, vol. 19, no. 5, pp. 694–716, 2015.
- [45] S. Jiang and S. Yang, “A strength pareto evolutionary algorithm based on reference direction for multi-objective and many-objective optimization,” *IEEE Trans. Evolutionary Computation*, 2016, accepted for publication.
- [46] Y. Yuan, H. Xu, B. Wang, and X. Yao, “A new dominance relation-based evolutionary algorithm for many-objective optimization,” *IEEE Trans. Evolutionary Computation*, vol. 20, no. 1, pp. 16–37, 2016.
- [47] K. Li, S. Kwong, and K. Deb, “A dual-population paradigm for evolutionary multiobjective optimization,” *Inf. Sci.*, vol. 309, pp. 50–72, 2015.
- [48] Q. Zhang and H. Li, “MOEA/D: A multiobjective evolutionary algorithm based on decomposition,” *IEEE Trans. Evolutionary Computation*, vol. 11, no. 6, pp. 712–731, 2007.
- [49] K. Miettinen, *Nonlinear Multiobjective Optimization*. Kluwer Academic Publishers, 1999, vol. 12.
- [50] K. Miettinen and M. M. Mäkelä, “On scalarizing functions in multiobjective optimization,” *OR Spectrum*, vol. 24, no. 2, pp. 193–213, 2002.
- [51] R. Chen, K. Li, and X. Yao, “Dynamic multi-objectives optimization with a changing number of objectives,” *IEEE Trans. Evolutionary Computation*, 2017, accepted for publication.
- [52] M. Wu, S. Kwong, Q. Zhang, K. Li, R. Wang, and B. Liu, “Two-level stable matching-based selection in MOEA/D,” in *SMC’15: Proc. of the 2015 IEEE International Conference on Systems, Man, and Cybernetics*, 2015, pp. 1720–1725.
- [53] M. Wu, K. Li, S. Kwong, Y. Zhou, and Q. Zhang, “Matching-based selection with incomplete lists for decomposition multi-objective optimization,” *IEEE Trans. Evolutionary Computation*, 2017, accepted for publication.
- [54] K. Deb and R. B. Agrawal, “Simulated binary crossover for continuous search space,” *Complex Systems*, vol. 9, 1994.
- [55] K. Deb and M. Goyal, “A combined genetic adaptive search (GeneAS) for engineering design,” *Computer Science and Informatics*, vol. 26, pp. 30–45, 1996.
- [56] K. Deb, L. Thiele, M. Laumanns, and E. Zitzler, *Scalable Test Problems for Evolutionary Multiobjective Optimization*. London: Springer London, 2005, pp. 105–145.
- [57] S. Huband, P. Hingston, L. Barone, and R. L. While, “A review of multiobjective test problems and a scalable test problem toolkit,” *IEEE Trans. Evolutionary Computation*, vol. 10, no. 5, pp. 477–506, 2006.
- [58] H. Ishibuchi, Y. Setoguchi, H. Masuda, and Y. Nojima, “Performance of decomposition-based many-objective algorithms strongly depends on pareto front shapes,” *IEEE Trans. on Evolutionary Computation*, vol. 21, no. 2.

- [59] E. Zitzler and L. Thiele, “Multiobjective evolutionary algorithms: a comparative case study and the strength pareto approach,” *IEEE Trans. Evolutionary Computation*, vol. 3, no. 4, pp. 257–271, 1999.
- [60] R. Saborido, A. B. Ruiz, and M. Luque, “Global WASF-GA: An evolutionary algorithm in multiobjective optimization to approximate the whole pareto optimal front,” *Evolutionary computation*, pp. 1–41, 2016, accepted for publication.
- [61] Y. Xiang, Y. Zhou, M. Li, and Z. Chen, “A vector angle based evolutionary algorithm for unconstrained many-objective optimization,” *IEEE Trans. Evolutionary Computation*, vol. 21, no. 1, 2017.
- [62] X. Zhang, Y. Tian, and Y. Jin, “A knee point-driven evolutionary algorithm for many-objective optimization,” *IEEE Trans. Evolutionary Computation*, vol. 19, no. 6, pp. 761–776, 2015.
- [63] H. Wang, L. Jiao, and X. Yao, “Two_arch2: An improved two-archive algorithm for many-objective optimization,” *IEEE Trans. Evolutionary Computation*, vol. 19, no. 4, pp. 524–541, 2015.
- [64] H. Sato, “Inverted PBI in MOEA/D and its impact on the search performance on multi and many-objective optimization,” in *Genetic and Evolutionary Computation Conference, GECCO '14*, 2014, pp. 645–652.
- [65] K. Li, K. Deb, O. T. Altinöz, and X. Yao, “Empirical investigations of reference point based methods when facing a massively large number of objectives: First results,” in *EMO'17: Proc. of the 9th International Conference on Evolutionary Multi-Criterion Optimization*, 2017, pp. 390–405.